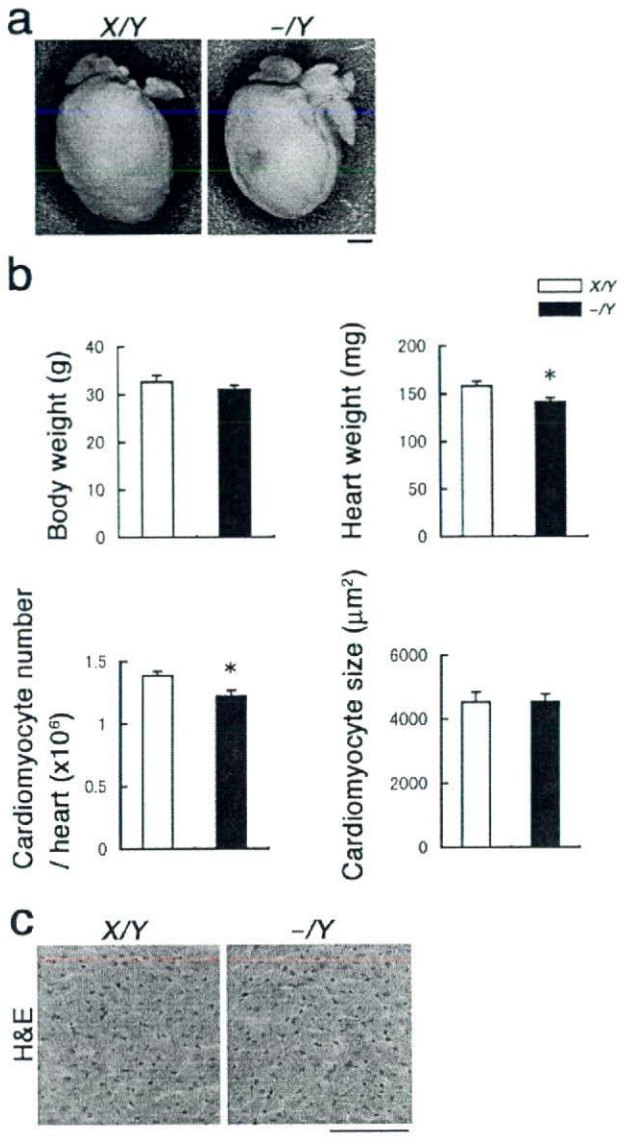

Fig. 3.

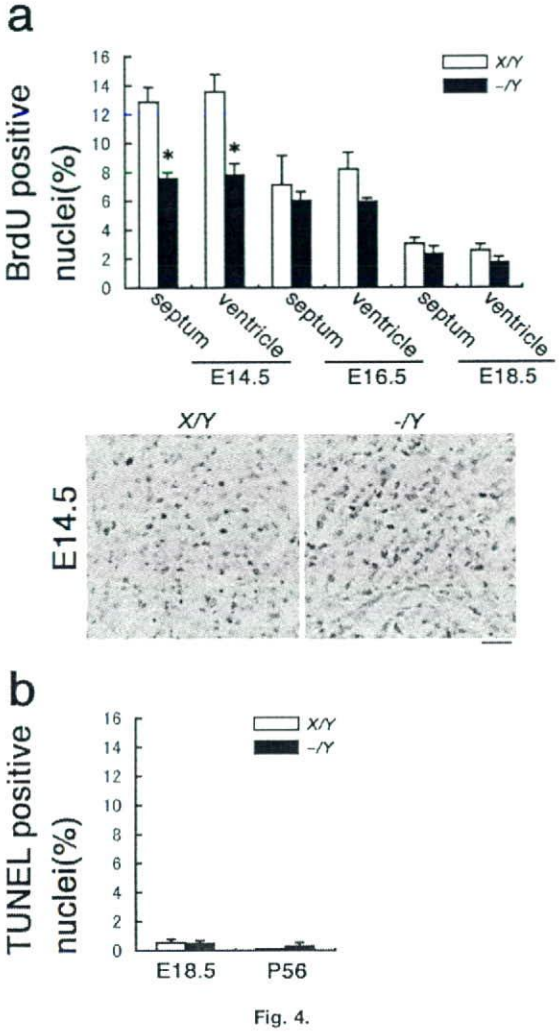

Fig. 4.

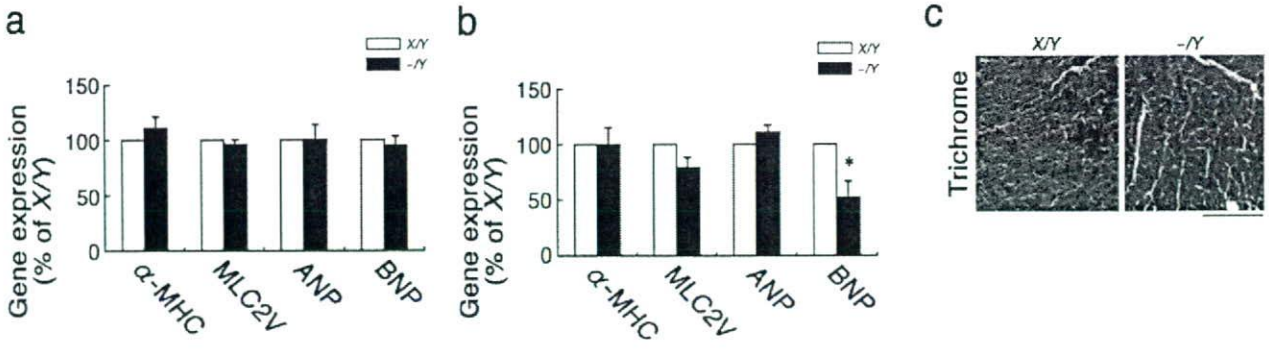

Fig. 5.

we examined the *Fgf16* knockout heart for fibrosis by conducting Masson trichrome staining. However, no cardiac fibrosis was found in the ventricles (Fig. 5c).

Fgf16 Knockout Heart Function

As described above, heart weight and the number of cardiomyocytes in *Fgf16* knockout mice were slightly but significantly reduced. These results indicate heart function to be impaired in *Fgf16* knockout mice. We examined tail-cuff systolic blood pressure at 6 months of age (Table 1). Blood pressure was essentially unchanged in *Fgf16* knockout mice. We also examined cardiac performance at 6 months of age by echocardiography (Table 1). Heart rate, fractional shortening (FS), and the ejection fraction (EF) were essentially unchanged in the *Fgf16* knockout heart. The diastolic interventricle septal wall thickness (IVSd) and diastolic left ventricle posterior wall thickness (LVPWd) were also essentially unchanged. However, the diastolic left ventricle internal dimension (LVDd) was slightly but significantly decreased. This is consistent with the finding that the *Fgf16* knockout heart was slightly but significantly smaller than the wild-type heart.

TABLE 1. Blood Pressure and Echocardiographic Parameters in *Fgf16* Knockout Mice

	X/Y	*−/Y*
Blood pressure		
Systolic blood pressure (mmHg)	101.7 ± 5.0	97.3 ± 3.4
Diastolic blood pressure (mmHg)	52.5 ± 2.3	51.0 ± 2.2
Echocardiographic parameters		
Heart Rate (beats/min)	635 ± 19	625 ± 29
FS (%)	37.00 ± 0.86	40.57 ± 1.09
EF (%)	75.17 ± 0.91	79.00 ± 1.25
IVSd (mm)	0.92 ± 0.06	0.87 ± 0.05
LVPWd (mm)	0.85 ± 0.04	0.87 ± 0.04
LVDd (mm)	3.63 ± 0.13	3.27 ± 0.12*

Results are expressed as means ± SEM for *X/Y* (n = 6) and *−/Y* (n = 7) mice at 6 months of age. EF, ejection fraction; FS, fractional shortening; IVSd, diastolic interventricle septal wall thickness; LVPWd, diastolic left ventricle posterior wall thickness, LVDd; diastolic left ventricle internal dimension. *X/Y*, wild-type male; *−/Y*; knockout male. An asterisk indicates statistical significance compared with the wild-type (*$p < 0.07$).

DISCUSSION

Most *Fgf* genes have been disrupted in mice. The phenotypes of *Fgf* knockout mice indicate that Fgf signaling plays crucial roles in development and metabolism (Itoh and Ornitz, 2008). Although the expression profile of *Fgf16* and the activity of recombinant Fgf16 in vitro suggest potential roles for Fgf16 in the heart and brown adipose tissue (Miyake et al., 1998; Konishi et al., 2000; Sontag and Cattini, 2003), the actual roles in vivo remain unclear. In this study, we examined roles of Fgf16 in vivo by generating *Fgf16* knockout mice by homologous recombination. Although most tissues examined in these mice were essentially normal, heart weight and the number of cardiomyocytes were slightly but significantly decreased.

Cardiomyocytes mostly proliferate at embryonic stages (Pasumarthi and Field, 2002). During the postnatal pe-

Fig. 3. Analysis of *Fgf16* knockout mice. **a:** The heart in wild-type and *Fgf16* knockout male mice at 6 months of age. The *Fgf16* knockout heart was apparently normal. X/Y, wild-type male; *−/Y*; knockout male. **b:** Body weight, heart weight, cardiomyocyte number, and cardiomyocyte size in wild-type and *Fgf16* knockout male mice at 6 months of age. Body weight was essentially unchanged in the *Fgf16* knockout mice. In contrast, heart weight was slightly but significantly decreased. The number of cardiomyocytes was also slightly but significantly decreased. However, the size of cardiomyocytes was essentially unchanged. Results are expressed as means ± SEM for X/Y (n = 12) and *−/Y* (n = 14) embryos. Asterisks indicate statistical significance compared with the wild-type (*$P < 0.05$). **c:** The heart in wild-type and *Fgf16* knockout male mice at 6 months of age was examined by histological analysis with hematoxylin–eosin staining (H&E). No necrosis or cardiomyocyte disarray was observed in the *Fgf16* knockout heart. Scale bar = 1 mm in a; 100 μm in c.

Fig. 4. Proliferation and survival of cadiomyocytes in *Fgf16* knockout mice. **a:** The proliferation of cardiomyocytes in the septa and ventricles of the *Fgf16* knockout heart at embryonic day (E) 14.5, E16.5, and E18.5 was determined by the incorporation of bromodeoxyuridine (BrdU) into cardiomyocytes. The proliferation was significantly decreased in both the septum and the ventricle wall. Results are expressed as means ± SEM for X/Y at E14.5 (n = 4), X/Y at E16.5 (n = 4), X/Y at E18.5 (n = 5), *−/Y* at E14.5 (n = 7), *−/Y* at E16.5 (n = 2), and *−/Y* at E18.5 (n = 5). Asterisks indicate statistical significance compared with the wild-type (*$P < 0.05$). **b:** The survival of cardiomyocytes was examined by terminal deoxynucleotidyl transferase–mediated deoxyuridinetriphosphate nick end-labeling (TUNEL) assay. The number of TUNEL-positive cells was essentially unchanged in the *Fgf16* knockout heart at E18.5 and postnatal day (P) 56. Results are expressed as means ± SEM for X/Y at E18.5 (n = 4), X/Y at P56 (n = 3), *−/Y* at E18.5 (n = 5), and *−/Y* at P56 (n = 3). X/Y, wild-type male; *−/Y*; knockout male. Scale bar = 10 μm in a.

Fig. 5. Cardiac marker gene expression and histopathological analysis in *Fgf16* knockout heart. **a:** The expression of cardiac marker genes in the *Fgf16* knockout heart at embryonic day (E) 18.5 was examined by reverse transcriptase-polymerase chain reaction (RT-PCR). The expression of all cardiac marker genes examined was essentially unchanged. X/Y, wild-type male; *−/Y*; knockout male. *α-MHC*, *α-myosin heavy chain*; *MLC2V*, *myosin light chain 2V*; *ANP*, *atrial natriuretic peptide*; *BNP*, *brain natriuretic peptide*. **b:** The expression of cardiac marker genes in the *Fgf16* knockout heart at 6 months of age was also examined. The expression of *α-MHC*, *MLC2V*, and *ANP* was essentially unchanged. In contrast, the expression of *BNP* was significantly decreased. Results are expressed as means ± SEM for X/Y at E18.5 (n = 7), X/Y at 6 months (n = 5), *−/Y* at E18.5 (n = 4), and *−/Y* at 6 months (n = 6). An asterisk indicates statistical significance compared with the wild-type (*$P < 0.05$). **c:** The *Fgf16* knockout heart at 6 months of age was examined by Masson trichrome staining (Trichrome). However, cardiac fibrosis was not found in the ventricles. Scale bar = 100 μm.

riod, cardiomyocytes stop proliferating and increase in size. Postnatal cardiac growth is mediated by cardiomyocyte hypertrophy (Li et al., 1996). Several studies using culture models suggest that Fgf signaling is involved in these developmental events. For example, exogenous Fgf2 promoted the proliferation of cardiomyocytes in culture (Kardami, 1990). However, heart development was not impaired in *Fgf2* knockout mice (Zhou et al., 1998). In contrast, Fgf9, which is a member of the *Fgf9/16/20* subfamily, plays a role in the proliferation of embryonic cardiomyocytes in vivo (Lavine et al., 2005). *Fgf9* knockout mice died shortly after birth (Colvin et al., 2001). The embryonic heart of *Fgf9* knockout mice was slightly smaller than that of wild-type mice. The proliferation of cardiomyocytes was significantly decreased in the *Fgf9* knockout heart at embryonic stages. The phenotype is similar to that of the *Fgf16* knockout heart. Furthermore, both recombinant Fgf9 and Fgf16 had a proliferative effect on heart explants in vitro (Lavine et al., 2005). In addition, Fgf9 and Fgf16 potentially share similar biochemical properties (Ornitz and Itoh, 2001; Zhang et al., 2006) and their expression profiles in the embryonic heart were similar. These findings suggest Fgf9 and Fgf16 to synergistically promote the proliferation of embryonic cardiomyocytes. We also examined the expression of *Fgf9* in the *Fgf16* knockout heart at E18.5. However, the expression was essentially unchanged (data not shown).

Fgf signaling is also thought to be involved in the acquisition of cardiac fate. For example, Fibroblast growth factor receptor 1 (Fgfr1) is essential for the development of cardiomyocytes in vitro (Dell'Era et al., 2003). The disruption of both *Fgfr1* and *Fgfr2* in the embryonic mouse heart resulted in cellular hypertrophy (Lavine et al., 2005). Therefore, we examined the differentiation of cardiomyocytes in the embryonic *Fgf16* knockout heart. However, the expression of cardiac markers, α-*MHC*, *MLC2V*, and *ANP*, was essentially unchanged, indicating that Fgf16 is not required for the differentiation of embryonic cardiomyocytes. In addition, no obvious abnormality was observed in the *Fgf16* knockout heart by histological analysis.

Fgf16 was also expressed in the postnatal heart, indicating potential roles for Fgf16. The decreased heart weight and the decreased number of cardiomyocytes in *Fgf16* knockout mice indicate heart function to be impaired. However, blood pressure and cardiac performance were essentially normal in *Fgf16* knockout mice, indicating that heart function was not impaired.

We also examined the expression of cardiac marker genes in the postnatal *Fgf16* knockout heart. Although the expression of α-*MHC*, *MLC2V*, and *ANP* was essentially unchanged, the expression of *BNP* was significantly decreased. Focal fibrotic lesions were observed in *BNP* knockout mice (Tamura et al., 2000). However, cardiac fibrosis was not found in the ventricles of any *Fgf16* knockout mice examined. Therefore, Fgf16 is not involved in cardiac fibrosis under physiological conditions. On the other hand, *BNP* expression is increased in the heart in response to pressure overload (Nakagawa et al., 1995). In the heart of *BNP* knockout mice, multifocal fibrotic lesions were significantly increased in size and number in response to ventricular pressure overload (Tamura et al., 2000). In addition, although the development of the heart was almost normal, *Fgf2* knockout mice developed significantly less hypertrophy than wild-type mice in response to pressure overload (Schultz et al., 1999). Therefore, Fgf16 might play roles in the heart under pathological conditions, including pressure overload and myocardial infarction.

In conclusion, Fgf16, which is expressed in cardiomyocytes, is a growth factor for embryonic cardiomyocytes, and may synergistically act with Fgf9.

EXPERIMENTAL PROCEDURES

Expression of *Fgf9*, *Fgf16* and *Fgf20* in Adult Tissues and Embryonic Heart Examined by RT-PCR

Total RNA was extracted from mouse tissues, cardiomyocytes, or noncardiomyocytes using an RNeasy mini kit (Qiagen). Cardiomyocytes and noncardiomyocytes were prepared from mouse neonatal hearts as described (Nakagawa et al., 1995). cDNA was synthesized from the RNA (1 μg) as a template in a reaction mixture containing moloney murine leukemia virus reverse transcriptase (Gibco BRL) and a random hexadeoxynucleotide primer (Takara, Japan). The cDNA was amplified by PCR with Taq DNA polymerase (Wako, Japan) and primers specific for *Fgf9* (sense primer, 5′-GTC CTC TGA TGG CTC CCT TA-3′; antisense primer, 5′-AGA CAC TGT CTT TGT CAG CTT-3′), *Fgf16* (sense primer, 5′-CCG CTT CGG AAT TCT GGA AT-3′; antisense primer, 5′-GGA CAT GGA GGG CAA CTT AGA A-3′) or *Fgf20* (sense primer, 5′-CCA TGG CTC CCT TGA CCG AA-3′; antisense primer, 5′-GGC TCT AGA TTC ATC AAG TG-3′). As a control, the expression of mouse *18S rRNA* was also examined by PCR using primers specific for *18S rRNA* (sense primer, 5′-CTT AGA GGG ACA AGT GGC G-3′; antisense primer, 5′-ACG CTG AGC CAG TCA GTG TA-3′). The PCR product was separated by electrophoresis on a 2% agarose gel, visualized by ethidium bromide staining, and quantified with Image J software.

Gene Targeting

Mouse *Fgf16* gene fragments, a 7.6-kbp fragment for the 5′ homology recombination arm and a 1.6-kbp fragment for the 3′ homology recombination arm, were amplified from the genomic DNA of 129 mouse embryonic stem (ES) cells as a template by PCR with KOD$^+$ DNA polymerase (TOYOBO). A targeting vector was constructed by ligation of the fragments, the 5′ and 3′ homology recombination arms and a 6.3-kbp fragment for an IRES-LacZ-polyA/PGK-neo cassette. A diphtheria toxin A (DTA) expression cassette was inserted at the 5′ end of the targeting vector (Ohbayashi et al., 2002). The coding region of the mouse *Fgf16* is divided into three exons, exons 1–3. Most of exon 2 and all of exon 3 of *Fgf16* were replaced with the IRES-LacZ-polyA/PGK-neo cassette. The targeting vector was linearized with *Not*I and electroporated into C57BL/6 ES cells. The selection in G418 produced five homologous recombinant ES cell clones that were confirmed by Southern blot analysis using a 3′ probe.

Mouse Fgf16 is located on chromosome X. Germ-line chimeras were produced by the simple aggregation method (Wood et al., 1993) with *Fgf16* disrupted ES (−/Y) cells and morulae isolated from 129 Sv mice. Male chimeras were mated with C57BL/6 females. All mice were housed in a temperature-controlled environment with a 12-hr light/dark cycle.

Genotyping of Mice

Genotypes of mice were determined by PCR using the following primers: P1 (5′-GTC TTG CCT CAC AAT CTA CC-3′), P2 (5′-CCC GTG ATA TTG CTG AAG AG-3′), and P3 (5′-TGG CCA GCC TCT TCA TTC TA-3′). P1 and P3 produced a 509-bp fragment of the wild-type *Fgf16* locus. P2 and P3 produced a 273-bp fragment of a mutant *Fgf16* locus. The sex was determined by PCR using primers specific for chromosome Y (sense primer, 5′-CGC CCT TTA ATA TCG AAT CAC-3′; antisense primer, 5′-TCC AGT TCA TTT AGC CTC TGA-3′).

Histological Analysis

The heart at 6 months of age was fixed overnight in 4% paraformaldehyde, dehydrated, embedded in paraffin, and sectioned at 6 μm. Sections were stained with hematoxylin and eosin or with Masson trichrome and examined by light microscopy.

Morphometric Measurement of Isolated Cardiomyocytes

Paraformaldehyde-fixed hearts (the atria were removed) were digested with 12.5 M KOH for 20 hr as previously described (Gerdes et al., 1998). After careful washing with phosphate-buffered saline, rod-shaped cells, cardiomyocytes, were examined by light microscopy, and counted using a hemocytometer. Images of cardiomyocytes were captured and cell areas were measured for at least 50 cells per mouse using ImageJ software.

Proliferation Analysis

Time-mated female embryos were injected IP with BrdU (100 μg / g body weight) 1 hr before killing. BrdU immunohistochemistry on sections was performed as described (Naski et al., 1998). Sections were counterstained with hematoxylin. The number of BrdU-positive nuclei relative to the total number of nuclei was counted.

TUNEL Analysis

The heart at E18.5 and P56 was fixed. Sections of the heart were prepared as described (Naski et al., 1998). Apoptotic cells on the sections were detected using a DeadEnd Colorimetric TUNEL System kit (Promega).

Expression of Genes in Heart Examined by Quantitative RT-PCR

Total RNA was prepared from mouse heart at E18.5 and 6 months of age using an RNeasy mini Kit (Qiagen). The expression of genes was examined by RT-PCR with Taq DNA polymerase (Wako, Japan) and primers specific for mouse *α-myosin heavy chain* (*MHC*; sense primer, 5′-AGA TGG CTG ACT TCG GGG CAG-3′; antisense primer, 5′-CAT GGC CAT GTC CTC GAT CTT GT-3′), *myosin light chain 2V* (*MLC2V*; sense primer, 5′-TGT TCC TCA CGA TGT TTG GG-3′; antisense primer, 5′-CTC AGT CCT TCT CTT CTC CG-3′), *atrial natriuretic peptide* (*ANP*) (sense primer, 5′-CGG TGT CCA ACA CAG ATC TG-3′; antisense primer, 5′-AAG CTG TTG CAG CCT AGT CC-3′), *brain natriuretic peptide* (*BNP*; sense primer, 5′-GAT CTC CTG AAG GTG CTG TCC-3′; antisense primer, 5′-ATC CGG TCT ATC TTG TGC CCA-3′), and *18S rRNA*. The PCR product was separated by electrophoresis on a 2% agarose gel, visualized by ethidium bromide staining, and quantified with Image J software. As a control, the expression of mouse *18S rRNA* was also examined by RT-PCR using primers specific for *18S rRNA*.

Blood Pressure Measurement

The blood pressure of mice at 6 months of age was measured by the tail-cuff method (Nakanishi et al., 2007). At least 20 readings were taken for each measurement, and each mouse was measured 5 times for 2 weeks.

Ecocardiography

Mice at 6 months of age were examined by conscious ecocardiography. During the echocardiography, the animals were restrained by grasping the skin on the back of the neck and wrapping the tail (Xu et al., 2007). Diastolic interventricle septal wall thickness (IVSd), diastolic left ventricle internal dimension (LVDd), diastolic left ventricle posterior wall thickness (LVPWd), fractional shortening (FS), ejection fraction (EF), and heart rate were calculated using the echocardiographic system (Toshiba Power Vision 8000) equipped with a 12-MHz imaging transducer (Nakanishi et al., 2007).

Statistical Analysis

Results are expressed as the mean ± standard error of measurement (SEM). The statistical significance of differences in mean values was assessed with Student's *t*-test.

ACKNOWLEDGMENTS

M.K and N.I. were funded by the Ministry of Education, Science, Culture, Sports, and Technology, Japan and N.I. was funded by the Takeda Science Foundation and the Mitsubishi Foundation.

REFERENCES

Argentin S, Ardati A, Tremblay S, Lihrmann I, Robitaille L, Drouin J, Nemer M. 1994. Developmental stage-specific regulation of atrial natriuretic factor gene transcription in cardiac cells. Mol Cell Biol 14:777–790.

Colvin JS, White AC, Pratt SJ, Ornitz DM. 2001. Lung hypoplasia and neonatal death in Fgf9-null mice identify this gene as an essential regulator of lung mesenchyme. Development 128:2095–2106.

Dell'Era P, Ronca R, Coco L, Nicoli S, Metra M, Presta M. 2003. Fibroblast growth factor receptor-1 is essential for in vitro cardiomyocyte development. Circ Res 93: 414–420.

Gerdes AM, Onodera T, Tamura T, Said S, Bohlmeyer TJ, Abraham WT, Bristow MR. 1998. New method to evaluate myocyte remodeling from formalin-fixed biopsy and autopsy material. J Card Fail 4:343–348.

Itoh N, Ornitz DM. 2004. Evolution of the Fgf and Fgfr gene families. Trends Genet 11:563–569.

Itoh N, Ornitz DM. 2008. Functional evolutionary history of the mouse Fgf gene family. Dev Dyn 237:18–27.

Kardami E. 1990. Stimulation and inhibition of cardiac myocyte proliferation in vitro. Mol Cell Biochem 92:129–135.

Konishi M, Mikami T, Yamasaki M, Miyake A, Itoh N. 2000. Fibroblast growth factor-16 is a growth factor for embryonic brown adipocytes. J Biol Chem 275: 12119–12122.

Lavine KJ, Yu K, White AC, Zhang X, Smith C, Partanen J, Ornitz DM. 2005. Endocardial and epicardial derived FGF signals regulate myocardial proliferation and differentiation in vivo. Dev Cell 8:85–95.

Li F, Wang X, Capasso JM, Gerdes AM. 1996. Rapid transition of cardiac myocytes from hyperplasia to hypertrophy during postnatal development. J Mol Cell Cardiol 28:1737–1746.

Lyons GE, Schiaffino S, Sassoon D, Barton P, Buckingham M. 1990. Developmental regulation of myosin gene expression in mouse cardiac muscle. J Cell Biol 111: 2427–2436.

Miyakawa K, Imamura T. 2003. Secretion of FGF-16 requires an uncleaved bipartite signal sequence. J Biol Chem 278: 35718–35724.

Miyake A, Konishi M, Martin FH, Hernday NA, Ozaki K, Yamamoto S, Mikami T, Arakawa T, Itoh N. 1998. Structure and expression of a novel member, FGF-16, on the fibroblast growth factor family. Biochem Biophys Res Commun 243:148–152.

Nakagawa O, Ogawa Y, Itoh H, Suga S, Komatsu Y, Kishimoto I, Nishino K, Yoshimasa T, Nakao K. 1995. Rapid transcriptional activation and early mRNA turnover of brain natriuretic peptide in cardiocyte hypertrophy. Evidence for brain natriuretic peptide as an "emergency" cardiac hormone against ventricular overload. J Clin Invest 96:1280–1287.

Nakanishi M, Harada M, Kishimoto I, Kuwahara K, Kawakami R, Nakagawa Y, Yasuno S, Usami S, Kinoshita H, Adachi Y, Fukamizu A, Saito Y, Nakao K. 2007. Genetic disruption of angiotensin II type 1a receptor improves long-term survival of mice with chronic severe aortic regurgitation. Circ J 71:1310–1316.

Naski MC, Colvin JS, Coffin JD, Ornitz DM. 1998. Repression of hedgehog signaling and BMP4 expression in growth plate cartilage by fibroblast growth factor receptor 3. Development 125:4977–4988.

Ohbayashi N, Shibayama M, Kurotaki Y, Imanishi M, Fujimori T, Itoh N, Takada S. 2002. FGF18 is required for normal cell proliferation and differentiation during osteogenesis and chondrogenesis. Genes Dev 16:870–879.

Ogawa Y, Nakao K, Mukoyama M, Shirakami G, Itoh H, Hosoda K, Saito Y, Arai H, Suga S, Jougasaki M. 1990. Rat brain natriuretic peptide-tissue distribution and molecular form. Endocrinology 126:2225–2227.

Ornitz DM, Itoh N. 2001. Fibroblast growth factors. Genome Biol REVIEWS2:3005.

Pasumarthi KB, Field LJ. 2002. Cardiomyocyte cell cycle regulation. Circ Res 90: 1044–1054.

Schultz JE, Witt SA, Nieman ML, Reiser PJ, Engle SJ, Zhou M, Pawlowski SA, Lorenz JN, Kimball TR, Doetschman T. 1999. Fibroblast growth factor-2 mediates pressure-induced hypertrophic response. J Clin Invest 104:709–719.

Sontag DP, Cattini PA. 2003. Cloning and bacterial expression of postnatal mouse heart FGF-16. Mol Cell Biochem 242:65–70.

Tamura N, Ogawa Y, Chusho H, Nakamura K, Nakao K, Suda M, Kasahara M, Hashimoto R, Katsuura G, Mukoyama M, Itoh H, Saito Y, Tanaka I, Otani H, Katsuki M. 2000. Cardiac fibrosis in mice lacking brain natriuretic peptode. Proc Natl Acad Sci U S A 97:4239–4244.

Thisse B, Thisse C. 2005. Functions and regulations of fibroblast growth factor signaling during embryonic development. Dev Biol 287:390–402.

Wood SA, Pascoe WS, Schmidt C, Kemler R, Evans MJ, Allen ND. 1993. Simple and efficient production of embryonic stem cell-embryo chimeras by coculture. Proc Natl Acad Sci U S A 90:4582–4585.

Xu Q, Ming Z, Dart AM, Du XJ. 2007. Optimizing dosage of ketamine and xylazine in murine echocardiography. Clin Exp Pharmacol Physiol 34:499–507.

Zhang X, Ibrahimi OA, Olsen SK, Umemori H, Mohammadi M, Ornitz DM. 2006. Receptor specificity of the fibroblast growth factor family. The complete mammalian FGF family. J Biol Chem 281:15694–15700.

Zhou M, Sutliff RL, Paul RJ, Lorenz JN, Hoying JB, Haudenschild CC, Yin M, Coffin JD, Kong L, Kranias EG, Luo W, Boivin GP, Duffy JJ, Pawlowski SA, Doetschman T. 1998. Fibroblast growth factor 2 control of vascular tone. Nat Med 4:201–207.

0013-7227/08/$15.00/0
Printed in U.S.A.

Endocrinology 149(2):483–491

doi: 10.1210/en.2007-1094

Therapeutic Potential of Atrial Natriuretic Peptide Administration on Peripheral Arterial Diseases

Kwijun Park, Hiroshi Itoh, Kenichi Yamahara, Masakatsu Sone, Kazutoshi Miyashita, Naofumi Oyamada, Naoya Sawada, Daisuke Taura, Megumi Inuzuka, Takuhiro Sonoyama, Hirokazu Tsujimoto, Yasutomo Fukunaga, Naohisa Tamura, and Kazuwa Nakao

Department of Medicine and Clinical Science, Kyoto University Graduate School of Medicine, Kyoto 606-8507, Japan

Peripheral arterial diseases are caused by arterial sclerosis and impaired collateral vessel formation, which are exacerbated by diabetes, often leading to leg amputation. We have reported that an activation of the natriuretic peptides/cGMP/cGMP-dependent protein kinase pathway accelerated vascular regeneration and blood flow recovery in murine legs, for which ischemia had been induced by a femoral arterial ligation as a model for peripheral arterial diseases. In this study, ip injection of carperitide, a human recombinant atrial natriuretic peptide, accelerated blood flow recovery with increasing capillary density in ischemic legs not only in nondiabetic mice but also in mice kept upon streptozotocin-induced hyperglycemia for 16 wk, which significantly impaired the blood flow recovery compared with nondiabetic mice. Based on these findings, we tried to apply the administration of carperitide to the treatment of peripheral arterial diseases. The study group comprised a continuous series of 13 patients with peripheral arterial diseases (Fontaine's classification I, one; II, five; III, two; and IV, five), for whom conventional therapies had not accomplished appreciable results. Carperitide was administrated continuously and intravenously for 2 wk to Fontaine's class I–III patients and for 4 weeks to class IV patients. The dose was gradually increased to the maximum, with the patient's systolic blood pressure being kept above 100 mm Hg. Carperitide administration improved the ankle-brachial pressure index, intermittent claudication, rest pain, and ulcers. In conclusion, this study showed a therapeutic potential of carperitide to treat peripheral arterial diseases refractory to conventional therapies. (*Endocrinology* 149: 483–491, 2008)

LOWER EXTREMITY PERIPHERAL artery disease (PAD), which consists of arteriosclerosis thrombosis and thromboangitis obliterans, is caused by the altered structure and function of the arteries that supply the lower limbs. Numerous pathophysiological processes can contribute to the creation of stenoses or aneurysms of peripheral artery circulation. Among them, diabetes mellitus is one of the most important causes of PAD. According to the Centers for Disease Control and Prevention's National Center for Chronic Disease Prevention and Health Promotion, 82,000 people have diabetes-related leg, foot, or toe amputations each year in the United States. World Diabetes Day announced that up to 70% of leg amputation cases are patients with diabetes. In PAD patients with diabetes, collateral vessel formation is impaired (1), and intricately modified angiogenesis contributes to a large variety of complications including diabetic gangrene (2). Mechanisms that alter angiogenesis in diabetes are largely unknown. It is reported, however, that either inappropriate production or action of nitric oxide (NO) may play important roles in vascular insufficiencies with diabetes (3). NO activates soluble guanylyl cyclase (GC) followed by the cGMP signal transduction cascade (4). Significant reverse correlation between the urinary cGMP excretion rate and the disease grade according to Fontaine's classification observed in PAD patients seems to imply the impact of diminished cGMP production in PAD (5).

Natriuretic peptides (NPs) consist of atrial NP (ANP), brain NP (BNP), and C-type NP (CNP) and elicit various biological effects by activating particulate GCs: GC-A is a receptor selective for ANP and BNP, and GC-B is a receptor selective for CNP (4, 6–8). One of the major mediators of cGMP signaling is cGMP-dependent protein kinase (cGK) (4). ANP and BNP are secreted mainly from the atrium and ventricle of the heart, respectively, and act as cardiac hormones (4, 6, 7). The clinical significance of NPs is already recognized in the diagnosis and treatment of congestive heart failure (CHF). Recombinant human ANP and BNP are used for treating CHF, with the main expectation of diuretic and natriuretic effects (9, 10).

Recently, NPs have been revealed to have various effects on cell survival, proliferation, and differentiation. We reported that ANP at a physiological concentration induces endothelial regeneration in the human coronary artery and umbilical vein through the activation of ERK and phosphatidylinositol 3-kinase/Akt pathways (11). We used genetically engineered mice that overexpress BNP and type I cGK (cGKI), or otherwise lack cGKI, and demonstrated that BNP can promote vascular regeneration and accelerate the restoration of blood flow after the removal of a hind-limb artery in mice through the activation of the GC-A/cGMP/cGKI

First Published Online November 8, 2007

Abbreviations: ABI, Ankle-brachial pressure index; ADMA, asymmetric dimethylarginine; ANP, atrial natriuretic peptide; BNP, brain natriuretic peptide; cGK, cGMP-dependent protein kinase; cGKI, type I cGMP-dependent protein kinase; CHF, congestive heart failure; CNP, C-type natriuretic peptide; EC, endothelial cell; ESRD, end-stage renal disease; GC, guanylyl cyclase; NP, natriuretic peptide; PECAM, platelet endothelial cell adhesion molecule-1; SMC, smooth muscle cell; STZ, streptozotocin; VEGF, vascular endothelial growth factor.

Endocrinology **is published monthly by The Endocrine Society (http://www.endo-society.org), the foremost professional society serving the endocrine community.**

pathway (12–14). Meanwhile, CNP, which is secreted from endothelial cells (ECs) and acts as an endothelium-derived relaxing peptide (15), also induces redifferentiation of vascular smooth muscle cells (SMCs) while accelerating reendothelialization and suppressing neointimal hyperplasia in vein grafting or balloon injuries in rabbits, which simulate atherosclerotic lesions in humans (16, 17). These observations indicate that GC-A/cGMP and GC-B/cGMP signaling cascades have potential to promote vascular regeneration in PAD and to inhibit the progression of atherosclerotic lesions. On the other hand, we have reported previously that endothelial CNP expression is progressively reduced in accordance with the severity of human coronary atherosclerosis (18), which indicates that not only NO/soluble GC/cGMP signaling but also CNP/GC-B/cGMP signaling might be impaired in PAD. Therefore, the restoration of intracellular cGMP levels by the activation of GC-A, the third signaling pathway using cGMP as the second messenger in vascular SMCs and ECs, could improve PAD.

In this context, we hypothesized that an administration of ANP or BNP could, at least partly, compensate for impaired angiogenesis due to diminished intracellular cGMP levels in PAD patients by an activation of GC-A. In Japan, carperitide, a recombinant human ANP, is already approved and widely used for the treatment of CHF. By contrast, nesiritide, a recombinant human BNP, has not been approved in Japan, and it cannot be applied to rodent models because amino acid sequences and molecular forms of BNP are quite different between humans and rodents. In the present study, we therefore examined the effect of carperitide on vascular regeneration in animal models with diabetes, and we further tried to determine safety and to investigate any possible therapeutic effects of carperitide in PAD patients.

Materials and Methods

Animals

C57BL/6 male mice (CLEA Japan, Inc., Tokyo, Japan) were used for experiments. Diabetes was induced in the mice by repetitive (once a day for 4–6 consecutive days) ip injections of streptozotocin (STZ) (Nacalai Tesque Inc, Kyoto, Japan; 65–100 mg/kg body weight in 200 μl of 10 mM sodium citrate buffer, pH 4.0) at 8 wk of age. Blood glucose concentrations were monitored weekly after STZ treatment with Dexter-ZII (Bayer Medical Ltd., Tokyo, Japan). Animals with blood glucose levels above 220 mg/dl at 2 wk after the first STZ injection were used as STZ-diabetic mice. Control mice received an equal volume of citrate buffer. Mice were used for experiments of limb ischemia at 4, 16, and 26 wk after the first injection of STZ or vehicle.

An animal model of limb ischemia was made by a ligation of one femoral artery. The blood flow in both legs was assessed with a laser Doppler perfusion image analyzer (Moor Instruments, Devon, UK), and the blood flow recovery was assessed by the ischemic limb to normal limb ratio of blood flow, as we described previously (14).

To assess the effect of carperitide, a recombinant human ANP (Daiichi Asubio Pharma Co., Ltd., Tokyo, Japan), on angiogenesis in ischemic limbs, the femoral artery ligation was carried out at 16 wk after the first injection of STZ or vehicle, and carperitide at a dose of 2.2 μg/kg·min or equal volume of water (vehicle) was administered continuously and ip via a microosmotic pump (Alzet model 1002D; Alzet Pharmaceuticals, Palo Alto, CA), which was implanted ip at 3 d after the femoral artery ligation. Pumps were renewed at d 14 after primary implantation. At 28 d from the femoral artery ligation, mice were euthanized by an overdose of pentobarbital injection, and the ischemic hind limb was isolated for the histological analysis.

All experimental procedures were performed according to Kyoto University standards for animal care.

Histological analysis

After fixation with 4% paraformaldehyde, ischemic lower legs were embedded in OCT compound (Sakura Finetechnical, Tokyo, Japan) and frozen at −80 C. Cryostat sections (4–8 μm thick) of the tissue were stained with a rat antimouse platelet EC adhesion molecule-1 (PECAM-1) antibody (item 553370; PharMingen, San Diego, CA). Four random fields on two different sections (3 mm apart) from each mouse were photographed with a digital camera (Olympus, Tokyo, Japan). By computer-assisted analysis using NIH IMAGE, capillary density was calculated as the mean number of capillaries stained with PECAM-1, as we described previously (14).

Patients

Participants were a series of 13 Japanese patients including 11 males and two females, aged 38–92 yr, who had already been diagnosed with PAD and hospitalized in our department from June 2003 to August 2005 (Table 1). Patients classified as Fontaine's classes II–IV or with characteristic symptoms of PAD were included. Diseases accompanying PAD were defined as follows: type 2 diabetes mellitus, following the diagnostic criteria of Japan Diabetes Society; hypertension, blood pressure is equal to or greater than 140/90 mm Hg; end-stage renal disease, chronic renal failure on indispensable renal replacement therapy; ischemic heart disease, history of angina pectoris or myocardial ischemia with or without present medication; CHF, past diagnosis of CHF with or without present medication; hyperlipidemia, low-density lipoprotein-cholesterol is equal to or greater than 140 mg/dl, or triglyceride is equal to or greater than 150 mg/dl; obesity, body mass index is greater than 25 kg/m^2. Exclusion criteria were contraindications for carperitide: possibility of immediate surgery, suffering from malignancy, febrility, an inability to declare subjective symptoms, pregnancy, or other unfavorable statuses. The study was conducted in accordance with the guidelines in the Declaration of Helsinki. The study protocol was approved by the Ethics Committee Graduate School and Faculty of Medicine, Kyoto University. Patients were fully informed of the aim of the study, and their written informed consent was obtained.

Procedure of carperitide administration to patients

Carperitide was administered continuously and iv for 2 wk for Fontaine I–III patients and for 4 wk for Fontaine IV patients in principle. The starting dose of 0.006 μg/kg·min was gradually increased as long as the systolic blood pressure remained above 100 mm Hg. The range of final

TABLE 1. Patients' characteristics

Characteristic	n
Sex	
Male	11
Female	2
Diagnosis	
Arteriosclerosis obliterans	12
Thromboangitis obliterans	1
Gangrene or ulcer(s)	4
Fontaine's classification	
I	1
II	5
III	2
IV	5
Other disorders	
Hypertension	12
Type 2 diabetes	11
ESRD	7
CHF	5
Ischemic heart disease	4
Hyperlipidemia	4
Obesity (BMI > 25)	3

Patients' mean ± SD age was 72 ± 15 yr. BMI, Body mass index.

doses of carperitide used in this study was 0.003–0.1 μg/kg·min. Drugs for injection such as prostaglandins were avoided during the carperitide administration. The administration was stopped and standard remedy performed if any unfavorable symptoms appeared.

Pain was assessed when present with a numerical rating scale from 0–10; grade 0 indicated no pain and grade 10 the strongest pain the patient could imagine. The ankle-brachial pressure index (ABI) was assessed by an automated measurement device (BP-203RPEII; Colin Medical Technology Corp., Aichi, Japan). An exercise tolerance test was carried out weekly for patients with intermittent claudication. Pain-free walking distance on a flat ground was assessed. A stair-climb test was performed when walking on flat ground did not induce claudication. The test assessed how many floors a patient could climb without pain on the stair of our internal medicine ward building. Blood sampling was performed immediately before the beginning of carperitide administration and weekly during the administration for routine blood examination. It was also performed to determine the plasma levels of ANP, cGMP, and vascular endothelial growth factor (VEGF).

Analysis of blood samples

The blood samples from mice were withdrawn in an ice-cold tube containing 0.5 M Na_2EDTA final concentration and mixed well. Aprotinin was added at 500 U/ml when a sample was used for human ANP measurement. The plasma was immediately isolated by a centrifugation and stored at −20 C until further processing. Plasma concentrations of cGMP, VEGF, and human ANP were analyzed by SRL, Inc. (Tokyo, Japan).

Statistical analysis

Results are presented as mean ± SEM unless otherwise indicated. The statistical significance of differences in means was evaluated by ANOVA supplemented with Fisher's least-significant difference in comparisons among three or more groups in animal experiments and by paired *t* tests between before and after the carperitide administration in the human study. A P value < 0.05 was considered significant.

Results

Animal experiments

Angiogenesis was impaired in diabetic mice

Blood glucose levels in STZ-diabetic mice, on which the hind-limb ischemia was induced at 4, 16, and 26 wk after STZ injections, were 354 ± 151 mg/dl (n = 9), 354 ± 38 mg/dl (n = 9), and 308 ± 23 mg/dl (n = 9), respectively, on the day of surgery. In control nondiabetic mice, blood glucose levels at 4 wk after the injection of vehicle were 139 ± 4 mg/dl (n = 6), 132 ± 2 mg/dl (n = 9), and 131 ± 4 mg/dl (n = 9) for mice operated at 4, 16, and 26 wk, respectively, after the vehicle injection.

At 4 wk after the induction of diabetes, blood flow recovery of the STZ-diabetic group was similar to that of nondiabetic controls (Fig. 1A). But after a long-term hyperglycemic state of 16 or 26 wk, recovery was suppressed in the STZ-diabetic group by 26 or 32%, respectively, when compared with the control mice (Fig. 1, B and C).

ANP administration restored angiogenesis in diabetic mice

To investigate whether ANP can improve the impairment of blood flow recovery, carperitide was administered to C57BL/6 mice in which femoral artery ligation was made after a 16-wk exposure to hyperglycemia.

Blood glucose levels at femoral artery ligation were 116 ± 4 mg/dl in the vehicle-treated nondiabetic group, 122 ± 3 mg/dl in the carperitide-treated nondiabetic group, 343 ± 42 mg/dl in the vehicle-treated STZ-diabetic group, and 366 ± 42 mg/dl in the carperitide-treated STZ-diabetic group. In nondiabetic mice, the carperitide administration significantly accelerated blood flow recovery compared with the vehicle-treated group. The ischemic/normal limb blood flow ratio measured at 21 d after the surgery was 0.58 ± 0.03 in the vehicle-treated nondiabetic group (n = 13) and was significantly augmented in the carperitide-treated nondiabetic group (0.74 ± 0.06, n = 7; $P < 0.05$). The accelerating effect of carperitide on blood flow recovery was also seen in STZ-diabetic mice. The ischemic/normal limb blood flow ratio at

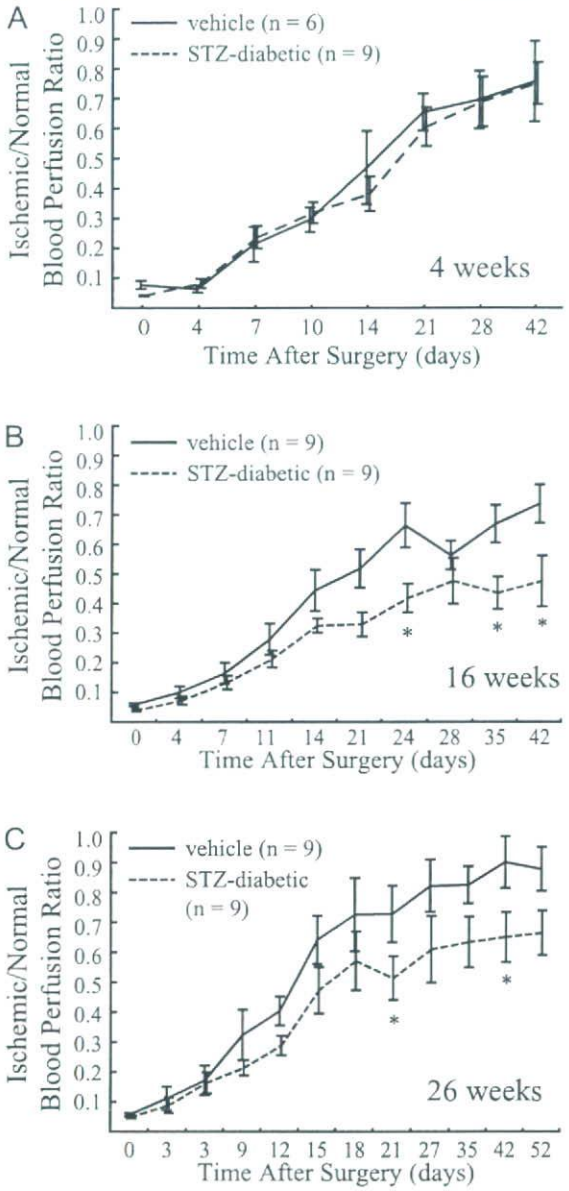

FIG. 1. Impairment of ischemia-induced blood flow recovery in mice with diabetes. Blood flow recovery after femoral artery ligation assessed by an ischemic/normal blood perfusion ratio was not altered 4 wk after STZ administration (A) but was significantly delayed 16 wk (B) and 26 wk (C) after induction of diabetes compared with vehicle-treated nondiabetic controls.*, $P < 0.05$ *vs.* vehicle-treated mice at each time point by ANOVA.

21 days after surgery was 0.52 ± 0.05 in the carperitide-treated STZ-diabetic group (n = 8) and significantly higher than that in the vehicle-treated STZ-diabetic group (0.37 ± 0.06, n = 7; $P < 0.05$) (Fig. 2B). The time course of blood flow recovery in each group was shown in Fig. 2A.

In the vehicle-treated STZ-diabetic group, the capillary density was 907 ± 69 counts/mm^2 (n = 6) and was more significantly reduced than in the vehicle-treated nondiabetic group (1406 ± 98 counts/mm^2, n = 6; $P < 0.05$) (Fig. 2, C and D). The capillary density tended to be higher in the carperitide-treated nondiabetic group (1604 ± 108 counts/mm^2, n = 6) than in the vehicle-treated nondiabetic group. Among STZ-diabetic mice, the carperitide administration significantly increased the capillary density to 1180 ± 95 counts/mm^2 (n = 6; $P < 0.05$).

In this study, 4-wk administration of carperitide to mice increased plasma human ANP levels from under the detection limit (10 pg/ml) to 156 ± 79 pg/ml (n = 5 each) and plasma cGMP levels from 8.9 ± 1.1 nM (n = 7) to 20.0 ± 2.9 nM (n = 6, $P < 0.05$). The carperitide administration altered blood pressure from 106 ± 3/73 ± 3 mm Hg to 94 ± 4/62 ± 4 mm Hg (n = 4 each; $P < 0.05$).

Human study

All patients had characteristic symptoms of PAD (Fontaine's class: I, one; II, five; III, two; and IV, five) (Table 2). A patient who was Fontaine's class I had a cold sensation in the lower extremities. The diagnosis was confirmed by ABI measurement, ultrasound velocity spectroscopy, or magnetic resonance angiography.

Hypertension and diabetes were the two most frequent underlying diseases among participants (Table 1). Among diabetic subjects, HbA1c levels were 7.7 ± 0.5%, and disease duration was 16.5 ± 2.1 yr. Seven patients suffered from end-stage renal diseases and were on hemodialysis. Eight patients had a past history of an ischemic heart disease, CHF, or both, and all of them were in stable condition with or without medication Plasma ANP levels were 315 ± 130 pg/ml, and ejection fractions measured by ultrasonic echocardiography were 49.9 ± 6.2%.

Plasma ANP levels were elevated from 224 ± 93 pg/ml at baseline to 400 ± 125 pg/ml during the administration (n = 12; $P < 0.05$; data were lacking in patient 5). Plasma cGMP levels were elevated from 14.4 ± 3.5 to 24.0 ± 4.5 nM (n =

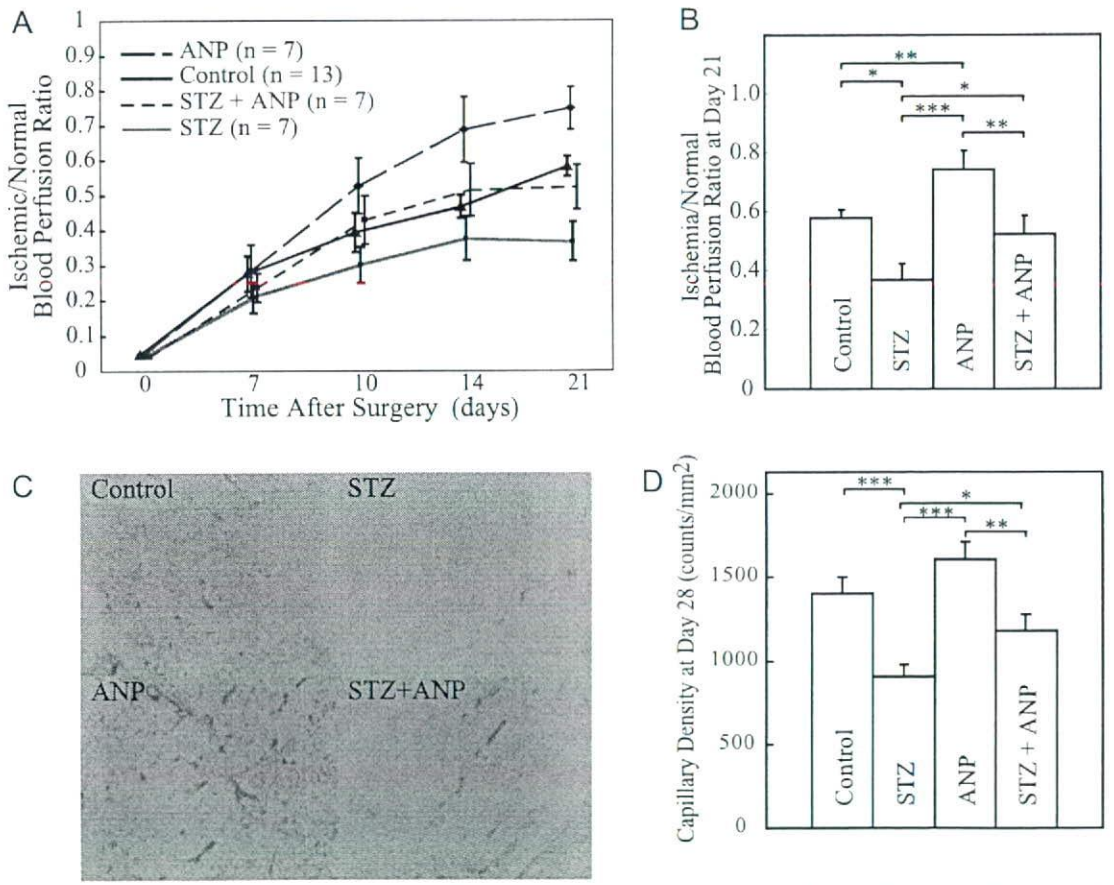

FIG. 2. Acceleration of ischemia-induced vascular regeneration by continuous ip administration of carperitide in nondiabetic and diabetic mice. A, Time course of ischemic/normal blood perfusion ratios measured by laser Doppler imaging; B, Calculated ischemic/normal blood perfusion ratios on d 21; C, immunostaining of the ischemic hind-limb tissue with anti-PECAM-1 antibody (*bright red*) at 28 d after the induction of ischemia; D. quantitative analysis of capillary density assessed by the immunostaining of PECAM-1. Control, Vehicle-treated nondiabetic; STZ, vehicle-treated STZ-diabetic; ANP, carperitide-treated nondiabetic; STZ + ANP, carperitide-treated STZ-diabetic. *, $P < 0.05$; **, $P < 0.01$; ***, $P < 0.001$.

TABLE 2. Detailed patients' characteristics

Patient no.	Diagnosis	Age (yr)/sex	Fontaine's class	Accompanying disease	Symptoms	RP rating	Exercise tolerance	Plasma ANP levels (pg/ml)	Medication
1	ASO	69/M	III	ESRD, DM, HT, IHD	RP	3	NA	79	Ap, P, C
2	TAO	38/F	II	DM, Ob	IC	NA	290	<5	Ap, P, V
3	ASO	82/F	I	DM, HT, Ob, HL, CHF	CS	NA	NA	16	An, Ap, P, V
4	ASO	77/M	IV	ESRD, HT, CHF	Ul/RP	5	NA	668	An, Ap, P
5	ASO	90/M	IV	DM, HT	Ul/RP	4	NA	152	P, V
6	ASO	85/M	IV	ESRD, DM, HT	Ul/RP	NA	NA	51	An, C, N, V
7	ASO	76/M	II	DM, HT, Ob, HL	IC	NA	240	22	An, Ap, V
8	ASO	75/M	II	DM, HT, HL, IHD	IC	4	200	36	An, Ap, P, V
9	ASO	63/M	III	ESRD, HT	RP	NA	NA	97	An, Ap, P, V
10	ASO	92/M	II	ESRD, DM, HT, CHF	IC	NA	100	922	Ap, N, P
11	ASO	71/M	IV	ESRD, DM, HT, CHF	Ul	NA	NA	645	Ap
12	ASO	57/M	II	DM, HT, HL, IHD	IC	3	5F	14	Ap, C, V
13	ASO	55/M	IV	ESRD, DM, HT, CHF, IHD	Ul/RP		NA	137	An, Ap, P, V

For patient 12, exercise tolerance was assessed by a stair-climb test, the floor number of stair-climbing without pain was 5. Medications were continued during carperitide injection without a change. An, Angiotensin-converting enzyme inhibitor or angiotensin receptor blocker; Ap, antiplatelet; ASO, arteriosclerosis obliterans; C, cilostazaol; CS, cold sensation of the peripheral; DM, type 2 diabetes mellitus; F, female; 5F, five floors; HL, hyperlipidemia; HT, hypertension; IC, intermittent claudication; IHD, ischemic heart disease; M, male; N, nitrate; NA, not applicable; Ob, obesity; P, prostanoid; RP, rest pain; TAO, thromboangitis obliterans; Ul, gangrane or non-healing ulcer(s); V, vasodilator.

9; $P < 0.01$). No significant differences were seen in plasma VEGF levels: 92.2 ± 25.4 pg/ml at the baseline and 65.2 ± 11.1 pg/ml in the course of administration (n = 8). The blood pressure of patients (excepting those on hemodialysis) fell from 143 ± 8/74 ± 2 mm Hg to 123 ± 7/69 ± 3 mm Hg (n = 5; $P < 0.05$). An excessive decrease in systolic blood pressure to less than 90 mm Hg was observed in a few patients on hemodialysis and could be quickly reversed by reducing the carperitide infusion rate. Medications except for injections were continued during carperitide injection without any changes. Details of medications especially for PAD are shown in Table 2. Alprostadil (prostaglandin E) had been iv administrated daily for a week to patients 2 and 3, and for a month to patients 6 and 11, and was stopped at least 3 d before the beginning of carperitide administration. Phosphodiesterase inhibitors other than cilostazaol were not used in patients enrolled in this study. Smoking status was not changed in five never-smokers (patients 1, 3, 5, 12, and 13) and seven former smokers (patients 2, 4, 7, 8, 9, 10, and 11) during this study. One patient (no. 6) was a current smoker (20 cigarettes/d) at the enrollment and stopped smoking 7 d before the administration.

The ABI of the affected limb (or worse side when both limbs affected) was significantly elevated from 0.61 ± 0.08 at the baseline to 0.72 ± 0.09 on the 14th day of administration (n = 12; $P < 0.05$) except for patient 5, for whom the administration was stopped within a week (Table 3 and Fig. 3b). Brachial systolic blood pressure values for ABI calculations before and on the 14th day of administration were 140 ± 10 and 132 ± 8 mm Hg, respectively (n = 12; $P = 0.5$). Ankle systolic blood pressure values at affected limb were 84 ± 13 mm Hg before administration and were increased to 94 ± 11 mm Hg on the 14th day of administration (n = 12; $P = 0.4$).

Pain was assessed with a numerical rating scale in six patients who complained of rest pain (Table 2). Rest pain disappeared in three of the six patients (patient 6, 4/0; patient 9, 4/0; and patient 13, 3/0, as before/after the administration of carperitide) and was reduced in another patient (no. 1, 3/1). In patient 4, although the pain once worsened in the early phase of administration (from 4 to 6), the injections were continued, and the pain was reduced to level 1 within a week. In another patient (no. 5), the carperitide infusion was stopped at d 7 because rest pain had worsened (4 to 6) (Fig. 3A). All patients who felt the rating score of rest pain reduced could stop to use pain relievers or hypnotics.

Exercise performance was carried out on all patients with intermittent claudication except for those who could not walk as a result of rest pain or weakness (patients 2, 7, 8, 10, and 12) (Fig. 3C). The pain-free walking distance was assessed in four patients and prolonged in all of them after the carperitide administration (patient 2, 290 to 380 m; patient 7, 240 to 560 m; patient 8, 200 to 800 m; patient 10, 100 to 200 m). In another patient with a stair-climb test, the floor number of pain-free stair climbing was increased from five to seven.

Five patients had multiple foot ulcers, and dermatologists in our hospital had recommended foot amputation. Al-

TABLE 3. Changes in ABI by 14 d administration of carperitide

Patient no.	Systolic BP (mm Hg)				ABI	
	Brachial		Ankle			
	Before	2 wk	Before	2 wk	Before	2 wk
1	96	182	35	106	0.36	0.58
2	141	101	115	89	0.82	0.88
3	159	140	69	81	0.43	0.58
4	88	115	83	140	0.94	1.22
5	138	NA	86	NA	0.62	NA
6	176	151	188	154	1.07	1.02
7	150	123	112	108	0.75	0.88
8	113	117	97	78	0.86	0.67
9	162	100	0	0	0	0
10	101	99	60	90	0.59	0.91
11	143	161	66	111	0.46	0.69
12	153	132	80	83	0.52	0.63
13	201	164	107	91	0.53	0.55
Mean	140	132	84	94	0.61	0.72
(SEM)	10	8	13	11	0.08	0.09

Values of brachial and ankle brachial pressure and ABI in each patient before and on the d 14 of administration. The administration was interrupted on the d 7 in patient 5. Data of patient 5 are excluded for the calculation of mean and SEM. NA, Not assessed.

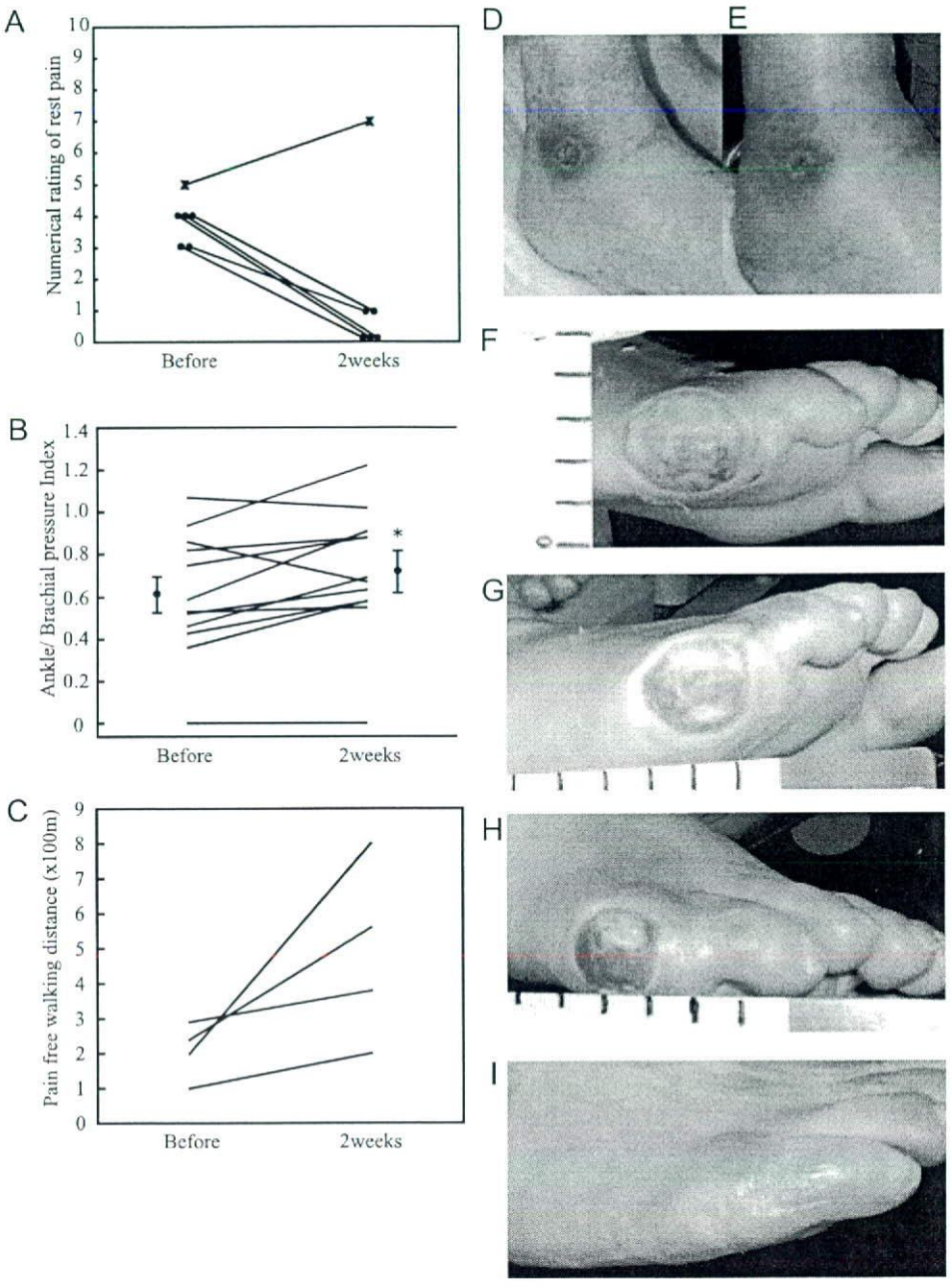

FIG. 3. Changes in symptoms resulting from carperitide infusion. A, Changes of 11-grade numerical rating of rest pain; B, changes in ABI of affected or worse side limb in each patient. Mean values are shown together with *error bars* (SEM) before and 2 wk after the carperitide administration. n = 12; *, $P < 0.05$. The administration was interrupted on the seventh day in patient 5, and ABI was undetectable in the affected limb of patient 9. C, Change in exercise tolerance assessed by pain-free walking distance; D–I, improvement of foot ulcer in patients 4 and 13. Pictures are before (D) and after 8-wk administration of carperitide (E) in patient 4 and before (F) and after 3 (G) and 6 (H) wk administration of carperitide and 4 months after leaving hospital (I) in patient 13. Pitting foot edema was observed in patient 4 (E).

though the ulcers did not change in severity in two cases (patients 5 and 6), they improved in another three cases (patients 4, 11, and 13) for whom foot amputations could be avoided. A representative case is shown in Fig. 3, D–I.

Other changes observed during administration were as follows: hot sensation in lower extremities in eight patients (nos. 1, 2, 4, 5, 6, 7, 8, and 13), transient flush and slight nausea in one patient (no. 2), pitting edema in both feet in five patients on hemodialysis (nos. 1, 4, 6, 11, and 13), and an increase in menstrual bleeding in a patient (no. 2).

Discussion

Diabetic foot is one of the most severe complications of diabetes mellitus and often results in leg amputation. Because it has been shown that an impairment of angiogenesis in patients with diabetes mellitus is a major cause of diabetic gangrene, we tried to generate a mouse model to investigate the mechanism of the impaired angiogenesis in diabetes. We induced diabetes in mice with STZ injections, and the mice were subjected to a femoral artery ligation after exposure to diabetic conditions (a blood glucose level higher than 220 mg/dl) for 4–26 wk. Although a 4-wk exposure to the diabetic condition did not affect blood flow recovery after the femoral artery ligation, exposure to high blood glucose for longer periods (16 or 26 wk) significantly impaired the blood flow recovery. This observation suggests that a quite long period of high blood glucose level is required to impair ischemia-induced collateral vessel formation. We therefore

selected 16 wk after the STZ induction of diabetes as the time point when the femoral artery ligation was performed on mice.

We showed here that carperitide, a recombinant human ANP, significantly accelerated blood flow recovery in a mouse model of ischemia-induced angiogenesis in both nondiabetic and diabetic conditions. The blood flow recovery in carperitide-treated diabetic mice was improved to a level similar to that in vehicle-treated nondiabetic mice. A histological analysis revealed that capillary density in the muscle of the ischemic limb was reduced in diabetic mice. The carperitide infusion significantly recovered capillary density in diabetic mice to the level in vehicle-treated nondiabetic mice. These observations indicate that carperitide can improve ischemia-induced angiogenesis, which accelerates blood flow recovery in diabetic conditions. We have shown that an increase of circulating BNP levels by targeted overexpression of the murine BNP gene in the liver or an overexpression of cGK throughout the body by the transgenic technology can accelerate the restoration of blood flow in limb ischemia experimentally generated by a femoral artery ligation, which results from the promotion of ischemia-induced angiogenesis through the activation of the ERK cascade (14). We have also shown that ANP at a physiological concentration induces proliferation and migration of ECs and enhances endothelial regeneration via activating ERK1/2 and phosphatidylinositol 3-kinase/Akt pathways in an *in vitro* wound healing assay using the cells from either coronary arteries or umbilical veins of humans (11). CNP, another member of the NP family, was shown to enhance migration of ECs and to accelerate reendothelialization in vein grafts after an arterial bypass surgery, although CNP inhibits proliferation and migration of vascular SMCs (16, 17). NPs use particulate GCs as their signaling receptors and share cGMP signaling pathways, especially signaling through cGKI, with NO, which activates soluble GC to generate cGMP (4). It is known that NO is a mediator of VEGF, which is a potent mitogen for vascular ECs and induces angiogenesis (19). A significant portion of VEGF-induced human EC proliferation is reportedly mediated by cGKI (20). In diabetes, hyperglycemia induces formation of reactive oxygen species, which decrease the bioavailability of NO (21). Taken together, deterioration of cGMP signaling appears to be a key process leading to the impaired angiogenesis and PAD in diabetes. In this study, the administration of carperitide could overcome the impairment of cGMP signaling in diabetic conditions, and it would be a new, therapeutic approach to PAD with diabetes. Because the urinary cGMP excretion rate is inversely correlated with the grade of Fontaine's classification in PAD patients (5), an impairment of cGMP signaling appears to be a common feature of PAD. We therefore investigated the therapeutic potential of carperitide administration in PAD patients.

We did not assign participants to a vehicle-treated group for an ethical reason; most cases of participants had been treated with conventional therapies, which had not accomplished appreciable effects. The carperitide administration significantly increased ABI, effectively relieved symptoms including intermittent claudication and rest pain, and promoted the healing of foot ulcers in PAD patients. The dosage of carperitide we used in the human study was optimized for each patient according to the maximum permissible dosage, which is the highest dose possible without causing an excessive fall in systolic blood pressure, because sensitivity to exogenously administered ANP differs among patients depending, presumably, upon basal plasma ANP levels. Although doses of carperitide administration were lower than those usually given in the treatment of CHF, plasma cGMP levels were increased twice as much as basal levels, and relief from the characteristic signs and symptoms of PAD became possible. This observation suggests that a blood pressure fall would not limit the therapeutic use of carperitide for PAD patients.

It is reported that asymmetric dimethylarginine (ADMA), an endogenous inhibitor of endothelial NO synthase, is accumulated in patients with end-stage renal disease (ESRD) and a high plasma ADMA level is a strong indicator of risks for all-cause mortality and cardiovascular events (22). It might be speculated that responses to the carperitide administration are better in ESRD patients than in non-ESRD patients, because carperitide is supposed to restore cGMP signaling, which is impaired by ADMA, via an activation of GC-A. Considering heterogeneity of patients' clinical characteristics, a larger number of participants will be needed to address this issue.

All patients, for whom exercise tolerance was evaluated, had been treated with conventional therapies using per os and per cutaneous medications under hospitalization and been encouraged to walk for at least 3 wk without any increases of pain-free walking distances. A 2-wk carperitide administration was then added to the conventional therapies and resulted in significantly improved exercise tolerance. The improvement, therefore, cannot be explained by a training effect only.

NPs have various biological effects on vascular functions other than the promotion of angiogenesis, and some of them appear favorable to treating PAD. NPs regulate vascular tone, and CNP, especially, is a candidate for endothelial-derived hyperpolarizing factor, which plays a fundamental role in the regulation of local blood flow and systemic blood pressure (23). In the clinical investigation of this paper, changes in symptoms and ABI appeared within a few days or a week of the administration. The effect of carperitide on symptoms in the early phase might be due to a vasodilatory action of ANP to some extent, because the changes appeared too early to be regarded as effects of vascular regeneration. On the other hand, the elongation of pain-free walking distance persisted after the cessation of the administration was ceased, and ABI remained elevated for several months after the end of administration. If the vasodilatory action of ANP is the only mechanism of the improvement, the effects of carperitide should disappear promptly at the cessation of the infusion, because the half life of ANP in circulation is a couple of minutes (24).

In patients with advanced arteriosclerosis, severe calcification of arterial walls in lower extremities can cause an overestimation of ankle blood pressure. Where vasodilators such as carperitide were used in such patients, ABI might be increased solely due to a decrease in brachial blood pressure. In this study, we observed slight decreases in brachial blood

pressure, but we could observe increases in ankle blood pressure although the changes were not statistically significant. Increases in ABI, therefore, should not be false and should be, at least in part, the result of blood flow recovery.

The improvement in exercise tolerance and ABI might, therefore, be achieved by modifying vascular endothelial structure or promoting vascular regeneration. Plasma VEGF levels were not significantly elevated by the carperitide infusion in this study, indicating that VEGF is not an essential mediator of carperitide's effects on PAD symptoms. It is reported that NPs elicit antiinflammatory and antithrombotic effects in animals (17, 25, 26), and further investigation will be needed to see whether such effects of NPs are clinically significant.

Carperitide is often used to treat CHF patients in Japan, and its safety is clinically proven. No critical side effects were observed in this study. An increase in menstrual bleeding observed in a participant could be accidental or a result of ANP's vasodilatory action, because the symptom faded soon after the cessation of the infusion. There are, however, several reports indicating the physiological significance of CNP/GC-B signaling in the control of ovarian cycling (27, 28). A close observation would be needed where carperitide infusion would be applied to women of reproductive age for a long duration (more than 2 wk). Leg edema appeared in three patients, who were in relatively serious states of the foot disease. Many PAD patients develop postoperative edema after surgeries of revascularization (29), which indicates that they have circulatory inadequacy for autoregulating blood hydrostatic pressure. Because ANP reportedly plays an essential role in maintaining vascular permeability via GC-A on vascular ECs (30), edema might result from this direct action on vascular endothelium.

Conclusion

This study revealed that a long-duration diabetic condition impaired ischemia-induced angiogenesis and blood flow recovery in a mouse model of hind-limb ischemia and that ANP as a therapeutic agent for CHF can restore the ischemia-induced angiogenesis in diabetic mice. Based on this observation, we applied carperitide administration to 13 PAD patients and found that carperitide infusion at doses lower than those for CHF could safely improve signs and symptoms. Carperitide administration, therefore, can be a new therapeutic strategy for PAD, and it appears effective in patients for whom conventional therapies do not work well.

Acknowledgments

We thank our colleagues in Kyoto University Hospital for referring patients and assistance; the staff of the Institute of Laboratory Animals, Graduate School of Medicine, Kyoto University for animal care; Ms. Akane Nonoguchi for technical assistance; and Ms. Ayumi Ishida and Ms. Shiho Takada for secretarial assistance.

Received August 7, 2007. Accepted November 1, 2007.

Address all correspondence and requests for reprints to: Hiroshi Itoh, M.D., Ph.D., Department of Internal Medicine, Keio University School of Medicine, Shinanomachi, Shinjuku-ku, Tokyo 160-8582, Japan. E-mail: hiito@kuhp.kyoto-u.ac.jp.

This work was supported by the Kyoto University 21st Century Centers of Excellence Program "Integration of Transplantation Therapy and Regenerative Medicine"; Grant-in-Aid for Scientific Research from the Ministry of Health, Labor, and Welfare; the Ministry of Education, Culture, Sports, Science, and Technology and the Japan Smoking Foundation; Grant of Regenerative Medicine Realization Project of the Ministry of Education, Culture, Sports, Science, and Technology; Fifth Grant for Clinical Vascular Function from the Kimura Memorial Heart Foundation; Grant from Takeda Medical Foundation; Grant from Japan Foundation of Applied Enzymology; and the Research Grant for Cardiovascular Disease 19C-7 from the Ministry of Health, Labor, and Welfare.

Disclosure Statement: The authors of this manuscript have nothing to declare.

References

1. **Rivard A, Silver M, Chen D, Kearney M, Magner M, Annex B, Peters K, Isner JM** 1999 Rescue of diabetes-related impairment of angiogenesis by intramuscular gene therapy with adeno-VEGF. Am J Pathol 154:355–363
2. **Martin A, Komada MR, Sane DC** 2003 Abnormal angiogenesis in diabetes mellitus. Med Res Rev 23:117–145
3. **Tesfamariam B, Cohen RA** 1992 Free radicals mediate endothelial cell dysfunction caused by elevated glucose. Am J Physiol 263:H321–H326
4. **Tamura N, Chrisman TD, Garbers DL** 2001 The regulation and physiological roles of the guanylyl cyclase receptors. Endocr J 48:611–634
5. **Boger RH, Bode-Boger SM, Thiele W, Junker W, Alexander K, Frolich JC** 1997 Biochemical evidence for impaired nitric oxide synthesis in patients with peripheral arterial occlusive disease. Circulation 95:2068–2074
6. **Sugawara A, Nakao K, Morii N, Yamada T, Itoh H, Shiono S, Saito Y, Mukoyama M, Arai H, Nishimura K, Obata K, Yasue H, Ban T, Imura H** 1988 Synthesis of atrial natriuretic polypeptide in human failing hearts. Evidence for altered processing of atrial natriuretic polypeptide precursor and augmented synthesis of β-human ANP. J Clin Invest 81:1962–1970
7. **Mukoyama M, Nakao K, Hosoda K, Suga S, Saito Y, Ogawa Y, Shirakami G, Jougasaki M, Obata K, Yasue H, Kambayashi Y, Inoue K, Imura H** 1991 Brain natriuretic peptide as a novel cardiac hormone in humans. Evidence for an exquisite dual natriuretic peptide system, atrial natriuretic peptide and brain natriuretic peptide. J Clin Invest 87:1402–1412
8. **Suga S, Nakao K, Hosoda K, Mukoyama M, Ogawa Y, Shirakami G, Arai H, Saito Y, Kambayashi Y, Inouye K** 1992 Receptor selectivity of natriuretic peptide family, atrial natriuretic peptide, brain natriuretic peptide, and C-type natriuretic peptide. Endocrinology 130:229–239
9. **Colucci WS, Elkayam U, Horton DP, Abraham WT, Bourge RC, Johnson AD, Wagoner LE, Givertz MM, Liang CS, Neibaur M, Haught WH, LeJemtel TH** 2000 Intravenous nesiritide, a natriuretic peptide, in the treatment of decompensated congestive heart failure. Nesiritide Study Group. N Engl J Med 343:246–253
10. **Suwa M, Seino Y, Nomachi Y, Matsuki S, Funahashi K** 2005 Multicenter prospective investigation on efficacy and safety of carperitide for acute heart failure in the 'real world' of therapy. Circ J 69:283–290
11. **Kook H, Itoh H, Choi BS, Sawada N, Doi K, Hwang TJ, Kim KK, Arai H, Baik YH, Nakao K** 2003 Physiological concentration of atrial natriuretic peptide induces endothelial regeneration in vitro. Am J Physiol Heart Circ Physiol 284:H1388–H1397
12. **Ogawa Y, Itoh H, Tamura N, Suga S, Yoshimasa T, Uehira M, Matsuda S, Shiono S, Nishimoto H, Nakao K** 1994 Molecular cloning of the complementary DNA and gene that encode mouse brain natriuretic peptide and generation of transgenic mice that overexpress the brain natriuretic peptide gene. J Clin Invest 93:1911–1921
13. **Pfeifer A, Klatt P, Massberg S, Ny L, Sausbier M, Hirneiss C, Wang GX, Korth M, Aszodi A, Andersson KE, Krombach F, Mayerhofer A, Ruth P, Fassler R, Hofmann F** 1998 Defective smooth muscle regulation in cGMP kinase I-deficient mice. EMBO J 17:3045–3051
14. **Yamahara K, Itoh H, Chun TH, Ogawa Y, Yamashita J, Sawada N, Fukunaga Y, Sone M, Yurugi-Kobayashi T, Miyashita K, Tsujimoto H, Kook H, Feil R, Garbers DL, Hofmann F, Nakao K** 2003 Significance and therapeutic potential of the natriuretic peptides/cGMP/cGMP-dependent protein kinase pathway in vascular regeneration. Proc Natl Acad Sci USA 100:3404–3409
15. **Suga S, Nakao K, Itoh H, Komatsu Y, Ogawa Y, Hama N, Imura H** 1992 Endothelial production of C-type natriuretic peptide and its marked augmentation by transforming growth factor-β. Possible existence of "vascular natriuretic peptide system". J Clin Invest 90:1145–1149
16. **Doi K, Ikeda T, Itoh H, Ueyama K, Hosoda K, Ogawa Y, Yamashita J, Chun TH, Inoue, M, Masatsugu K, Sawada N, Fukunaga Y, Saito T, Sone M, Yamahara K, Kook H, Komeda M, Ueda M, Nakao K** 2001 C-type natriuretic peptide induces redifferentiation of vascular smooth muscle cells with accelerated reendothelialization. Arterioscler Thromb Vasc Biol 21:930–936
17. **Ohno N, Itoh H, Ikeda T, Ueyama K, Yamahara K, Doi K, Yamashita J, Inoue M, Masatsugu K, Sawada N, Fukunaga Y, Sakaguchi S, Sone M, Yurugi T, Kook H, Komeda M, Nakao K** 2002 Accelerated reendothelialization with suppressed thrombogenic property and neointimal hyperplasia of rabbit jugular vein grafts by adenovirus-mediated gene transfer of C-type natriuretic peptide. Circulation 105:1623–1626

18. **Naruko T, Ueda M, van der Wal AC, van der Loos CM, Itoh H, Nakao K, Becker AE** 1996 C-type natriuretic peptide in human coronary atherosclerotic lesions. Circulation 94:3103–3108
19. **Morbidelli L, Chang CH, Douglas JG, Granger HJ, Ledda F, Ziche M** 1996 Nitric oxide mediates mitogenic effect of VEGF on coronary venular endothelium. Am J Physiol 270:H411–H415
20. **Hood J, Granger HJ** 1998 Protein kinase G mediates vascular endothelial growth factor-induced Raf-1 activation and proliferation in human endothelial cells. J Biol Chem 273:23504–23508
21. **Ceriello A, Motz E** 2004 Is oxidative stress the pathogenic mechanism underlying insulin resistance, diabetes, and cardiovascular disease? The common soil hypothesis revisited. Arterioscler Thromb Vasc Biol 24:816–823
22. **Kielstein JT, Zoccali C** 2005 Asymmetric dimethylarginine: a cardiovascular risk factor and a uremic toxin coming of age? Am J Kidney Dis 46:186–202
23. **Chauhan SD, Nilsson H, Ahluwalia A, Hobbs AJ** 2003 Release of C-type natriuretic peptide accounts for the biological activity of endothelium-derived hyperpolarizing factor. Proc Natl Acad Sci USA 100:1426–1431
24. **Ingwersen SH, Jorgensen PN, Eiskjaer H, Johansen NL, Madsen K, Faarup P** 1992 Superiority of sandwich ELISA over competitive RIA for the estimation of ANP-270, an analogue of human atrial natriuretic factor. J Immunol Methods 149:237–246
25. **Kiemer AK, Vollmar AM** 2001 The atrial natriuretic peptide regulates the production of inflammatory mediators in macrophages. Ann Rheum Dis 60(Suppl 3):68–70
26. **Scotland RS, Cohen M, Foster P, Lovell M, Mathur A, Ahluwalia A, Hobbs AJ** 2005 C-type natriuretic peptide inhibits leukocyte recruitment and platelet-leukocyte interactions via suppression of P-selectin expression. Proc Natl Acad Sci USA 102:14452–14457
27. **Tamura N, Doolittle LK, Hammer RE, Shelton JM, Richardson JA, Garbers DL** 2004 Critical roles of the guanylyl cyclase B receptor in endochondral ossification and development of female reproductive organs. Proc Natl Acad Sci USA 101:17300–17305
28. **Acuff CG, Huang H, Steinhelper ME** 1997 Estradiol induces C-type natriuretic peptide gene expression in mouse uterus. Am J Physiol 273:H2672–2677
29. **Coats P, Wadsworth R** 2005 Marriage of resistance and conduit arteries breeds critical limb ischemia. Am J Physiol Heart Circ Physiol 288:H1044–H1050
30. **Sabrane K, Kruse MN, Fabritz L, Zetsche B, Mitko D, Skryabin BV, Zwiener M, Baba HA, Yanagisawa M, Kuhn M** 2005 Vascular endothelium is critically involved in the hypotensive and hypovolemic actions of atrial natriuretic peptide. J Clin Invest 115:1666–1674

Endocrinology **is published monthly by The Endocrine Society (http://www.endo-society.org), the foremost professional society serving the endocrine community.**

OPEN ACCESS Freely available online

PLoS one

Augmentation of Neovascularizaiton in Hindlimb Ischemia by Combined Transplantation of Human Embryonic Stem Cells-Derived Endothelial and Mural Cells

Kenichi Yamahara[1☯], Masakatsu Sone[1☯], Hiroshi Itoh[1,2*], Jun K. Yamashita[3], Takami Yurugi-Kobayashi[3], Koichiro Homma[2], Ting-Hsing Chao[4], Kazutoshi Miyashita[1,2], Kwijun Park[1], Naofumi Oyamada[1], Naoya Sawada[1], Daisuke Taura[1], Yasutomo Fukunaga[1], Naohisa Tamura[1], Kazuwa Nakao[1]

1 Department of Medicine and Clinical Science, Kyoto University Graduate School of Medicine, Kyoto, Japan, **2** Department of Internal Medicine, Keio University School of Medicine, Tokyo, Japan, **3** Laboratory of Stem Cell Differentiation, Stem Cell Research Center, Institute for Frontier Medical Science, Kyoto University, Kyoto, Japan, **4** Division of Cardiology, Department of Internal Medicine, National Cheng Kung University Medical Center, Tainan, Taiwan

Abstract

Background: We demonstrated that mouse embryonic stem (ES) cells-derived vascular endothelial growth factor receptor-2 (VEGF-R2) positive cells could differentiate into both endothelial cells (EC) and mural cells (MC), and termed them as vascular progenitor cells (VPC). Recently, we have established a method to expand monkey and human ES cells-derived VPC with the proper differentiation stage in a large quantity. Here we investigated the therapeutic potential of human VPC-derived EC and MC for vascular regeneration.

Methods and Results: After the expansion of human VPC-derived vascular cells, we transplanted these cells to nude mice with hindlimb ischemia. The blood flow recovery and capillary density in ischemic hindlimbs were significantly improved in human VPC-derived EC-transplanted mice, compared to human peripheral and umbilical cord blood-derived endothelial progenitor cells (pEPC and uEPC) transplanted mice. The combined transplantation of human VPC-derived EC and MC synergistically improved blood flow of ischemic hindlimbs remarkably, compared to the single cell transplantations. Transplanted VPC-derived vascular cells were effectively incorporated into host circulating vessels as EC and MC to maintain long-term vascular integrity.

Conclusions: Our findings suggest that the combined transplantation of human ES cells-derived EC and MC can be used as a new promising strategy for therapeutic vascular regeneration in patients with tissue ischemia.

Citation: Yamahara K, Sone M, Itoh H, Yamashita JK, Yurugi-Kobayashi T, et al (2008) Augmentation of Neovascularizaiton in Hindlimb Ischemia by Combined Transplantation of Human Embryonic Stem Cells-Derived Endothelial and Mural Cells. PLoS ONE 3(2): e1666. doi:10.1371/journal.pone.0001666

Editor: Tailoi Chan-Ling, University of Sydney, Australia

Received November 5, 2007; **Accepted** January 24, 2008; **Published** February 27, 2008

Funding: This work is supported by a grant-in-aid for scientific research (the Japanese Ministry of Education, Culture, Sports, Science and Technology), a research grant from them 21st COE Program for Integration of Transplantation Therapy and Regenerative Medicine (Japan Society for the Promotion of Science), a research grant from the Project for Development of Regenerative Medicine (the Japanese Ministry of Education, Culture, Sports, Science and Technology), and a research grant from the Japan Foundation for Aging and Health (the Japanese Ministry of Health, Labor and Welfare).

Competing Interests: The authors have declared that no competing interests exist.

*E-mail: hrith@sc.itc.keio.ac.jp

☯These authors contributed equally to this work.

Introduction

Embryonic stem (ES) cells, with their extensive regeneration potential and functional multilineage differentiation capacity, are now highlighted as promising cell sources for regenerative medicine. Previously we reported that mouse ES cells-derived vascular endothelial growth factor receptor-2 (VEGFR2) positive cells could differentiate into both endothelial cells (EC) and mural cells (MC) (pericytes and vascular smooth muscle cells) and reproduce the vascular organization process, which we termed "vascular progenitor cells (VPC)" [1]. Transplanted VPC into tumor-bearing nude mice were incorporated into blood vessels and significantly increased blood flow, which suggests that VPC might be useful for augmenting vessel growth in ischemic tissue [2].

We have demonstrated that human as well as monkey ES cells possessed different differentiation kinetics of VPC derived from mouse ES cells [3,4]. In contrast to mouse ES cells, undifferentiated human ES cells already expressed VEGFR2. After the induction of differentiation on OP9 feeder cells, VEGFR2 positive and tumor rejection antigen-1 (TRA1: a marker indicative of undifferentiated cell phenotype) negative cells appeared at day 8. We confirmed that VEGFR2 positive cells at this stage effectively differentiated into both VE-cadherin positive EC and α-smooth muscle actin (αSMA) positive MC to suffice as human VPC.

Human VPC-derived VEGFR2$^+$ VE-cadherin$^+$ cells, which were considered as EC at an early differentiation stage, formed a network structure on Matrigel-coated dishes.

Based upon these works, in the present study we transplanted human VPC-derived vascular cells; that is, EC and MC in a murine hindlimb ischemia model. By transplantation of these EC and MC differentiated from human VPC, we investigated whether and how they could be incorporated as EC and MC into the sites of neovascularization, compared to human peripheral blood and umbilical cord blood-derived endothelial progenitor cell (EPC) transplantation [5–7]. Furthermore, we specifically asked whether the combined transplantation of human VPC-derived EC and MC could induce stable vascular regeneration to achieve long-term vascular integrity.

Results

Characterization of Transplanted Human VPC-derived Vascular Cells

Flow cytometric analysis disclosed that 20–40% of expanded human VPC-derived EC retained the expression of the endothelial cell-related markers, including VE-cadherin, VEGFR2, CD34, CD31 and CD105, and all of the cells were negative for a panleukocyte marker CD45, monocyte/macrophage marker (CD11b), and stem/progenitor makers (AC133 and c-kit) (Figure 1a). By the double immunostaining of CD31 and αSMA, the cells negative for CD31 were exclusively positive for αSMA (Figure 1b), but weak or negative for staining with other MC markers, including calponin, smooth muscle myosin heavy chain 1 (SM1) and 2 (SM2) (data not shown).

Immunocytochemistry of expanded human VPC-derived MC revealed that all these cells were positive for αSMA, calponin, SM1 and SM2 (Figure 1c). Analysis by reverse transcription-polymerase chain reaction (RT-PCR) also confirmed that mRNA expressions of these MC markers were upregulated in human VPC-derived MC and negative in sorted VE-cadherin$^+$ fraction of expanded human VPC-derived EC (Figure 1d). Although cultured human aortic smooth muscle cells (hAoSMC) expressed a high level of h-caldesmon, its expression in human VPC-derived MC was not detected. Furthermore, mRNA for skeletal (myogenin and MyoD) or cardiac (cardiac troponin T (cTnT) and I (cTnI)) specific marker was not detected in human VPC-derived MC (Figure 1e).

Characterization of Transplanted Human EPC

Flow cytometric analysis of pEPC demonstrated that these cells mainly exhibited two light-scattering properties: one was consistent with a relatively large cell size (gate P1) and the other was found in a smaller gate P2 (Figure 2a). The P1-gated cells were positive for DiI-acLDL uptake and ulex-lectin binding (Figure 2b), and exhibited the reported EPC phenotype [6,8]. However, the smaller P2-gated cells were low positive for DiI-acLDL/ulex-lectin (Figure 2c). Therefore, we performed subsequent fluorescence activated cell sorter (FACS) analysis of pEPC on the P1-gated cells.

As shown in Figure 2d, nearly all pEPC expressed the hematopoietic markers CD45 (99.9%) and CD54 (99.9%) and the monocyte/macrophage markers CD14 (99.0%), CD11b (98.7%), and CD11c (98.9%). The monocyte/macrophage or endothelial markers CD31 (58.3%) and CD105 (70.1%) were also expressed. A much lower percentage of these cells expressed the endothelial cell-related markers VE-cadherin (1.6%), VEGFR2 (5.4%), and von Willebrand Factor (vWF) (0.3%), or the stem/progenitor cell markers AC133 (1.0%), c-kit (0.4%), and CD34 (0.2%).

Flow cytometric analysis of magnetic cell separation system (MACS)-sorted uEPC showed more than 80% of these cells were positive for CD34 (data not shown). Similar to pEPC, almost all CD34$^+$ fraction of uEPC expressed the hematopoietic markers CD45 (99.0%) and CD54 (84.9%) (Figure 2e). However, the expression of monocyte/macrophage markers was limited in uEPC (CD14 5.7%, CD11b 99.7%, CD11c 21.3%), and significant number of these cells was positive for the endothelial cell-related markers, including VE-cadherin (11.2%), VEGFR2 (8.1%), and vWF (7.9%). In addition, these CD34$^+$ uEPC expressed the stem/progenitor markers AC133 (80.6%) and c-kit (95.3%).

Long-term Improvement of Blood Flow of Ischemic Hindlimb by Human VPC-derived Vascular Cell Transplantation

To examine the comparative effectiveness of transplanted human VPC-derived vascular cells for vascular regeneration, we set up six groups as follows (Figure 3);

1) EC+MC group (n = 9): the mixture of 0.5×10^6 human VPC-derived EC and 0.5×10^6 MC, with the total cell number of 1×10^6,
2) EC group (n = 20): 0.5×10^6 human VPC-derived EC,
3) MC group (n = 18): 0.5×10^6 human VPC-derived MC,
4) uEPC group (n = 10): 1×10^6 umbilical cord-derived CD34$^+$ cells,
5) pEPC group (n = 16): 1×10^6 peripheral mononuclear cells (MNC)-derived EPC,
6) Control group (n = 17): only 100 μl PBS.

To analyze subcutaneous hindlimb perfusion, laser Doppler perfusion image (LDPI) analysis was performed (Figure 4a). Throughout the 42 day follow-up period, significantly accelerated limb perfusion improvement was observed in the VPC-derived EC+MC-transplanted group, compared to the EPC and control groups (Figure 4b, $P<0.001$ vs. control, pEPC, uEPC, and MC groups, $P = 0.002$ vs. EC group, repeated measures ANOVA followed by Bonferoni's multiple comparison test).

At day 14, blood flow of the mice transplanted with EPC (the ratio of ischemic/non-ischemic blood flow: 0.907 ± 0.058 in pEPC and 0.942 ± 0.075 in uEPC) ($P = 0.035$ and 0.028, compared to the control group), as well as MC (0.957 ± 0.056) ($P = 0.006$) and EC (0.901 ± 0.063) ($P = 0.032$) showed significant increase, compared to the control group (0.730 ± 0.042) (Figure 4b). In the EC+MC group, the ratio of ischemic/non-ischemic blood flow markedly elevated to 1.187 ± 0.083 ($P<0.0001$), compared to other groups.

Blood flow in the pEPC group, however, did not increase thereafter and no significant difference in the blood flow between the pEPC and control group was seen at days 28 and 42 (Figure 4b). In the uEPC group, significant blood flow recovery was seen at day 42 (0.990 ± 0.054) ($P = 0.009$), compared to the control group (0.749 ± 0.039). The blood flow in the VPC-derived vascular cells-transplanted groups progressively increased. At day 42, the calculated perfusion ratio of ischemic to non-ischemic hindlimb significantly elevated to 0.943 ± 0.057 for the MC ($P = 0.013$), 1.038 ± 0.059 for the EC ($P = 0.0002$), and 1.231 ± 0.067 for the EC+MC group ($P<0.0001$) compared to the control group (0.749 ± 0.039). Between the cell mixture transplantation (EC+MC) group and the single cell transplantation (EC or MC) groups, the blood flow of ischemic hindlimbs was significantly different at day 42 ($P<0.05$).

Effective Contribution of Human VPC-derived Vascular Cells for Vascular Regeneration

Fixed tissues harvested from ischemic hindlimbs at day 7 were inspected by the fluorescence stereomicroscope (Leica, Wetzlar,

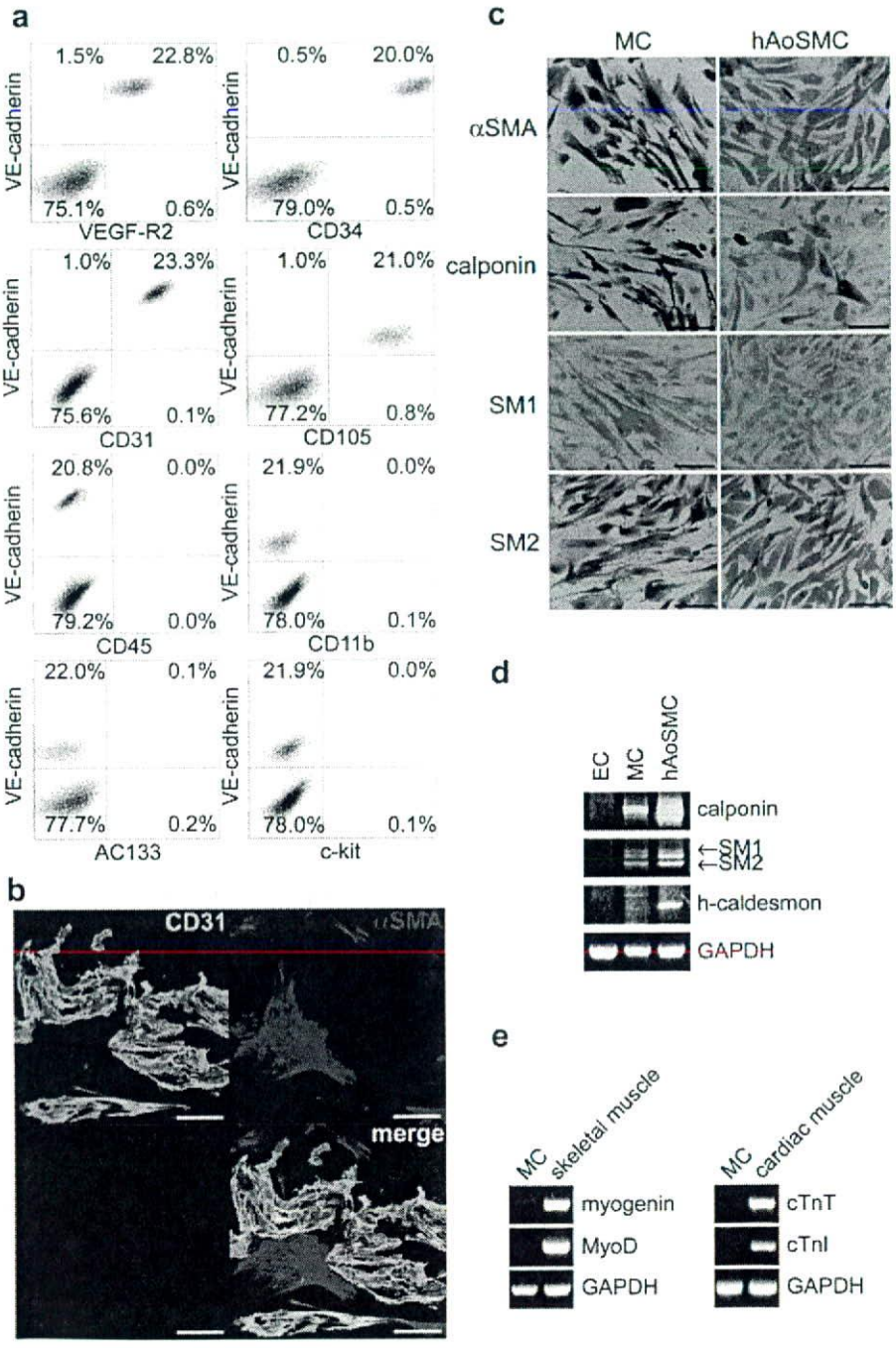

Figure 1. Characterization of transplanted human VPC-derived vascular cells. a) Flow cytometric analysis of cell surface markers on expanded human VPC-derived VEGF-R2$^+$VE-cadherin$^+$ cells (=EC). b) Immunofluorescence image of CD31 (green) and αSMA (red) with nuclear staining (blue) in expanded EC. Scale bar: 100 μm. c) Immunostaining of mural cell markers (brown) with hematoxyline counter-staining of expanded VPC-derived VEGF-R2$^+$VE$^-$cadherin- cells (=MC). Scale bar: 100 μm. d, e) RT-PCR analysis of mural cell (d) and skeletal/cardiac specific (e) markers in human VPC-derived vascular cells.
doi:10.1371/journal.pone.0001666.g001

Germany). Extended distribution of DiI-positive transplanted cells was clearly seen in both VPC-derived EC+MC and pEPC-transplanted hindlimbs (Figure 5a). We also detected some DiI-positive vessel-like formation in the lung and spleen, but no obvious tumor-like structures were seen (data not shown). Ischemic hindlimbs at day 14 were sectioned and treated with streptavidin conjugated dye to stain intravenously injected biotinylated isolectin B_4, followed by anti-human CD31 antibody, and scanned for the incorporation of transplanted cells into circulating vessels. In the EC+MC group, we found that human

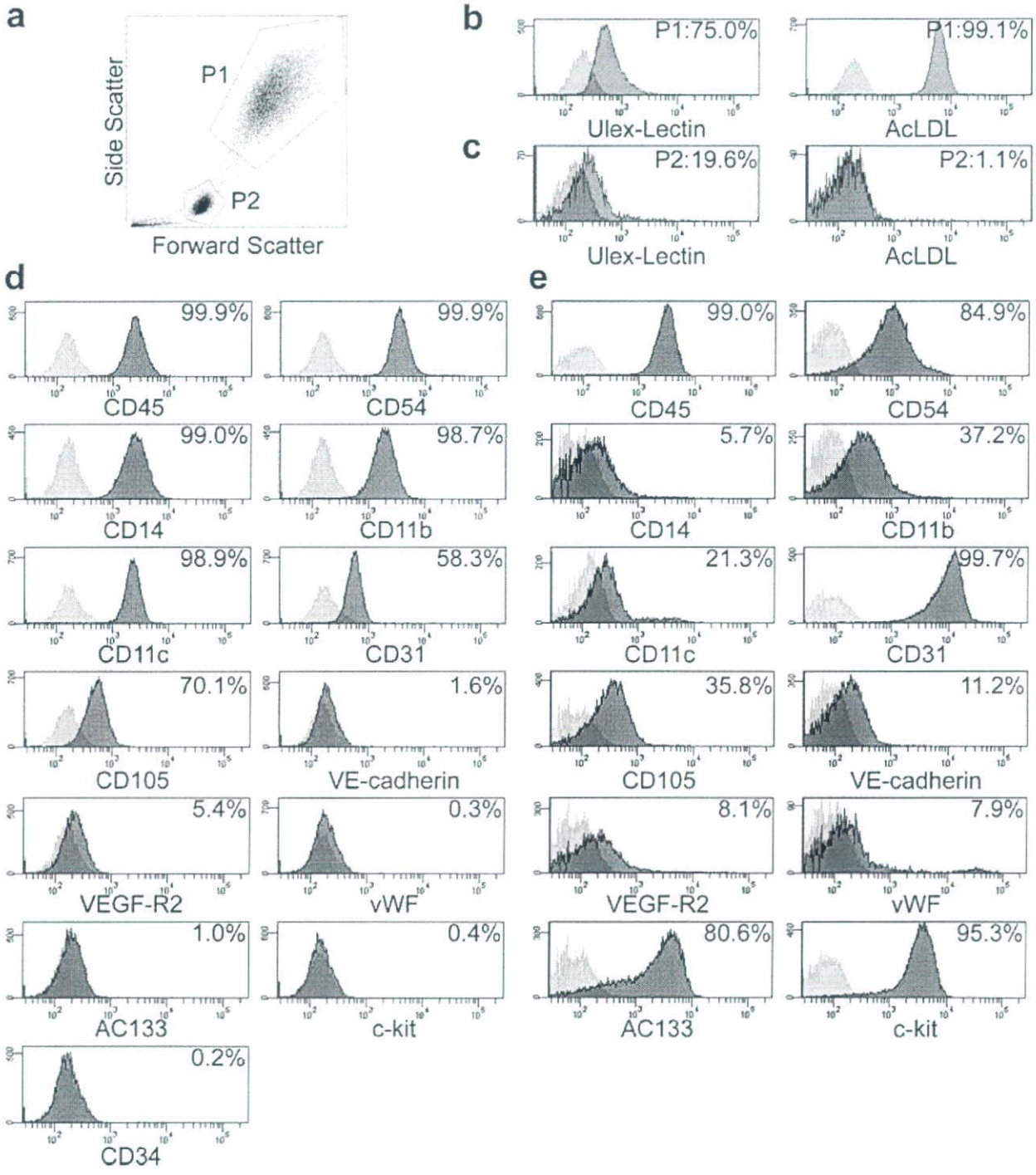

Figure 2. Characterization of peripheral blood and umbilical cord-derived EPC (pEPC and uEPC, respectively) by flow cytometer. a) Representative forward and side scatter profile of cultured pEPC. b-d) Flow cytometric analysis of ulex-lectin binding/acLDL uptake (b, c) and various cell surface markers (d) in pEPC. e) Flow cytometric analysis of cell surface markers in uEPC.
doi:10.1371/journal.pone.0001666.g002

CD31 positive cells formed capillaries with host EC, which were stained with isolectin B_4 (Figure 5b: arrowhead). Furthermore, some human CD31 positive cells solely formed capillary vessel (Figure 5b: arrow), which might indicate de novo vessel formation from human VPC-derived EC. We also detected human CD31 positive cells in the pEPC and uEPC group; however, many of these cells were located within the lumen of host capillaries (Figure 5c, arrow).

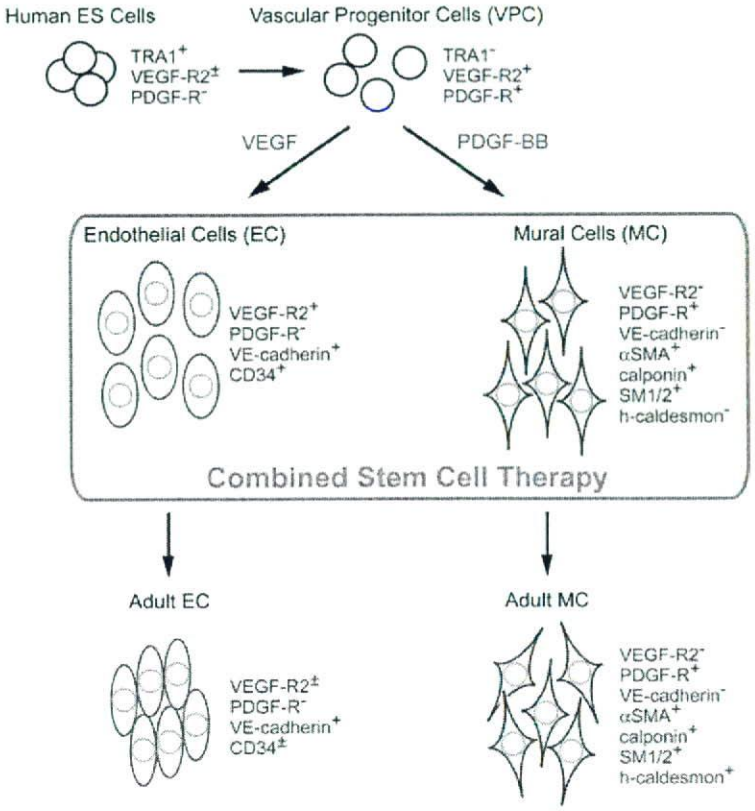

Figure 3. Possible differentiation pathway of vascular cells from human ES cells via VPC.
doi:10.1371/journal.pone.0001666.g003

We further investigated the contribution of transplanted VPC-derived MC to the recruitment of mural cells. We stained the sections of ischemic hindlimbs at day 14 with anti-human SM1 and αSMA antibodies. In EC+MC-transplanted mice, we found some human SM1 and αSMA double positive cells, which were localized within the αSMA positive host vessel wall (Figure 5d: arrow).

Quantification of Transplanted VPC-derived Vascular Cell-induced Vascular Regeneration in Ischemic Hindlimb

The sections of ischemic hindlimbs of the EC+MC group at day 42 were stained with anti-human and mouse CD31 antibodies. Mouse CD31 positive capillary density was significantly high in the EC+MC group ($1775.3\pm54.2/mm^2$), compared to other groups ($P<0.0001$ vs. control group: $1318.6\pm73.0/mm^2$) (Figure 6b). Human CD31 positive capillary density in mice transplanted with human VPC-derived EC (EC ($149.9\pm12.3/mm^2$) and EC+MC ($135.7\pm13.7/mm^2$) was significantly higher than that in mice transplanted with EPC ($95.7\pm8.5/mm^2$ in the pEPC and $115.2\pm12.0/mm^2$ in the uEPC group) ($P<0.05$). Compatible with the result of blood flow measurement, mouse and/or human CD31 positive capillary density markedly increased in mice that received human VPC-derived EC+MC ($1856.8\pm57.0/mm^2$) ($P<0.0001$, compared to the control group ($1318.6\pm73.0//mm^2$)), and also to other groups. Among the single cell transplantation groups, mouse and/or human CD31 positive capillary density increased in the EC group ($1601.4\pm51.4/mm^2$) ($P=0.0016$) compared to the control group, but did not increase in the MC ($1471.8\pm42.4/mm^2$) or EPC groups ($1403.5\pm84.4/mm^2$ in the pEPC and $1524.8\pm108.2/mm^2$ in the uEPC group).

To confirm the maturity of newly formed vessels, we performed the immunostaining of the ischemic tissues with anti-αSMA antibody, which could stain both human and mouse MC (Figure 6c). We confirmed that αSMA positive capillary density was significantly increased in the human VPC-derived vascular cells-transplanted groups (MC ($1317.6\pm45.4/mm^2$), EC ($1357.7\pm27.3/mm^2$) and EC+MC ($1554.9\pm48.8/mm^2$)) ($P<0.0001$), compared to the control group ($1021.3\pm46.3/mm^2$) (Figure 6d). Among the EPC groups, αSMA positive capillary density was significantly increased in the uEPC group ($1185.7\pm42.2/mm^2$) ($P<0.0076$) compared to the pEPC ($1118.9\pm36.8/mm^2$) and control group. We further investigated the extent of arteriogenesis in these groups using αSMA immunostaining sections. Many αSMA positive arterioles with more than 20 μm in diameter were detected in the EC+MC group, but not in the control group (Figure 6c: arrowhead). The number of αSMA positive arterioles significantly increased in the human VPC-derived vascular cells-transplanted groups, especially in the EC+MC group (the MC group:$4.0\pm0.3/mm^2$ and the EC group:$3.7\pm0.2/mm^2$; $P<0.001$, compared to the control group: $2.0\pm0.2/mm^2$, the EC+MC group: $5.5\pm0.7/mm^2$; $P<0.0001$, compared to all other groups) (Figure 6e). However, no significant difference in the number of αSMA positive arterioles was seen between the EPC (the pEPC group:$1.9\pm0.2/mm^2$ and the uEPC group:$2.0\pm0.2/mm^2$) and control groups.

Discussion

The present study demonstrated that the transplantation of human VPC-derived vascular cells at the proper differentiation

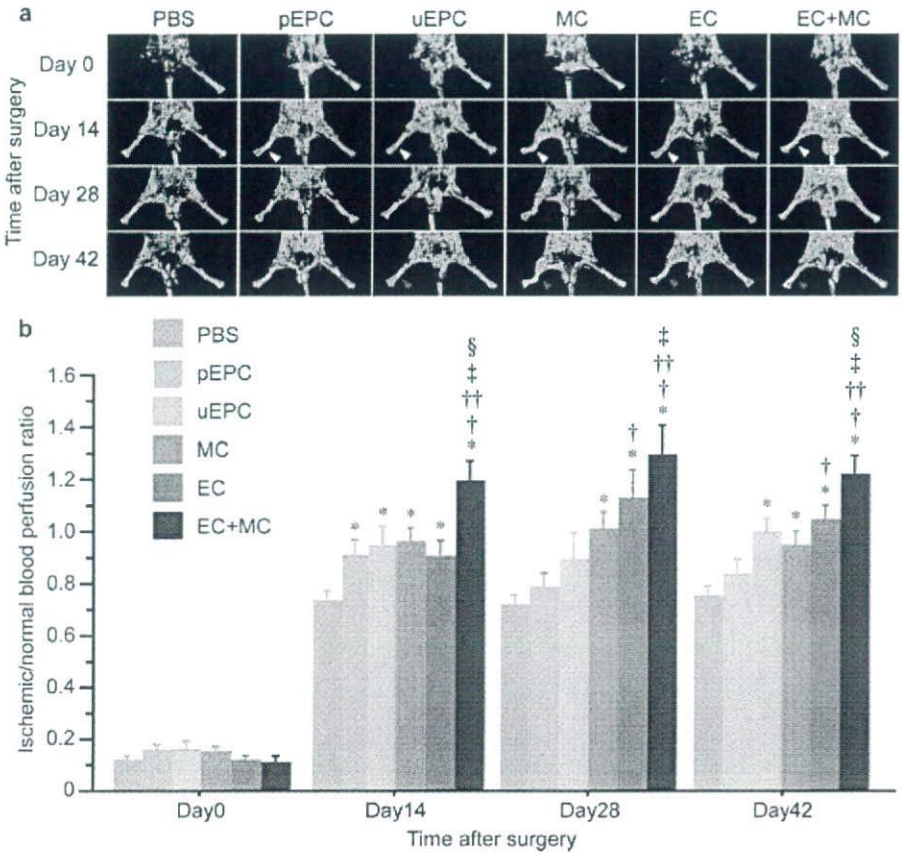

Figure 4. Augmented vascular regeneration by intra-arterial transplantation of human VPC-derived vascular cells in a murine hindlimb ischemia model. a) Serial LDPI analysis in hindlimb ischemia mice. At day 14, the blood flow of ischemic limbs in all cell transplanted groups increased significantly compared to the control group (white arrowhead). After 42 days, significant blood flow recovery was observed in the uEPC and human VPC-derived EC and/or MC-transplanted groups (red arrowhead), but not in pEPC. b) Quantitative analysis of hindlimb blood flow by calculating the ischemic/normal limb perfusion ratios after the induction of hindlimb ischemia. *$P<0.05$ vs. control, †$P<0.05$ vs. pEPC, ††$P<0.05$ vs. uEPC, ‡$P<0.05$ vs. MC, §$P<0.05$ vs. EC.
doi:10.1371/journal.pone.0001666.g004

stage successfully promoted vascular regeneration in the setting of tissue ischemia. After the expansion of human VPC-derived EC and MC, when intra-arterially administered, these cells significantly augmented neovascularization in an animal model of experimentally-induced hindlimb ischemia, compared to human peripheral blood and umbilical cord-derived EPC (pEPC and uEPC). Furthermore, the combined transplantation of human VPC-derived EC and MC could markedly induce vascular regeneration, compared to the single fraction transplantation of VPC-derived vascular cells (EC or MC). We also succeeded in demonstrating that transplanted human VPC-derived vascular cells were incorporated into the host circulation as both EC and MC. These results indicate that the combined transplantation of human VPC-derived EC and MC may have utility as a novel strategy for vascular regenerative medicine.

In the present study we used human VPC-derived VEGFR2$^+$ VE-cadherin$^+$ cells for the expansion and transplantation of EC. VEGFR2$^+$VE-cadherin$^+$ cells, obtained at day 10 of differentiation, were also positive for CD34 and therefore considered to be EC at the early differentiation stage (Figure 3) [9]. Even after 6 passages, 20~40% of these cells exhibited the expression of VEGFR2, VE-cadherin, and CD34, which indicated that they still retained the phenotype of EC at the early differentiated stage. Compared to EPC, transplantation of these EC significantly augmented ischemia-induced neovascularization. In contrast, we found that ischemia-induced neovascularization was not improved in mice receiving human aortic endothelial cells [4]. Therefore, human VPC-derived EC at the early differentiation stage might possess vascular regenerative capacity and these EC can be a valuable source for promoting vascular regeneration.

After expansion of human VPC-derived VEGFR2$^+$VE-cadherin$^+$ cells, about 70% of the expanded cells were αSMA positive. However, these cells were negative for the mature mural cell markers, including calponin, SM1, SM2, and h-caldesmon (data not shown). In contrast, expanded VEGFR2$^+$ VE-cadherin$^-$ cells obtained from human VPC under platelet derived growth factor (PDGF)-BB stimulation were positive for αSMA, calponin, SM1, and SM2, but negative for h-caldesmon. HAoSMC was positive for all of the mature MC markers, including h-caldesmon. In another series of our experiments, the mice receiving hAoSMC transplantation exhibited no significant improvement of neovascularization after the induction of ischemic hindlimbs (data not shown). Because h-caldesmon and calponin were reported to be expressed relatively late in SMC differentiation [10], human VPC-derived MC might be at a rather early "immature" differentiation